

Kishan prajapati

Condition monitoring and HI construction of bearings using vibration signals analysis.

Master's thesis in Reliability, Availability, Maintainability, and Safety (RAMS)

March 2021

Kishan prajapati

Condition monitoring and HI construction of bearings using vibration signals analysis.

Master's thesis in Reliability, Availability, Maintainability, and Safety
(RAMS)

Supervisor: Jørn Vatn

Co-supervisor: Bahareh Tajiani

March 2021

Norwegian University of Science and Technology

Faculty of Engineering

Department of Mechanical and Industrial Engineering



Norwegian University of
Science and Technology

Preface

This report is submitted as the master's thesis of an MSc degree, Reliability, Availability, Maintainability, and Safety (RAMS) for the study program TPK4950 Reliability, Availability, Maintainability, and Safety, Master's Thesis. It is carried out by Kishan Prajapati during the autumn semester of 2020. It is particularly focused on the vibration analysis for the extraction of health features and construction of health indicators of a roller bearing using time-frequency domain signal processing.

The project is connected to an ongoing PhD research carried out by a PhD candidate, Bahareh Tajiani. The report aims to perform an analysis of the lifetime vibration data of the bearings which are collected in the RAMS laboratory at Norwegian University of Science and Technology (NTNU) in Trondheim in Norway to construct the health indicators of the bearings which can be used for diagnosis and prognosis of the bearings. The data processing is done by one of the advanced time-frequency signal processing techniques named as Hilbert-Huang transform (HHT).

The report is targeted to the students and researchers who are researching for the development of a model for monitoring performance and RUL estimation of the roller bearings. The readers of the report should know the condition monitoring and maintenance strategies.

Trondheim, 31 – March-2021

Kishan Prajapati

Acknowledgment

I am grateful to my supervisor, Professor Jørn Vatn, and co-supervisor, Bahareh Tajiani, PhD candidate who provided useful sights, supports, and guidance while performing the project. I am equally grateful to Mr. Viggo Gabriel Borg Pedersen who provided information and knowledge about the RAMS laboratory for the vibration data collection of the roller bearings.

I would like to thank Øyvind Haave, RAMS laboratory and workshop manager for providing me access to collect the vibration samples of the bearing. I would also like to thank other contact persons like Bjørn Martin Bendixen and Arild Sæther who have helped me to unlock the RAMS laboratory.

Additional thanks to prof. Jørn Vatn and my close friends for providing me emotional supports throughout the project. And a special thanks to Lars Espen Bjørgum, advisor of faculty of science at NTNU for showing consideration towards me and providing me an extension for the master's thesis.

Finally, I would like to thank my parents and my siblings for providing supports and encouragement throughout the work.

K.P

Abstract

A bearing is one of the important components in rotatory machines and has been widely used in various industries. It plays a critical role in the rotating machines. The functionality and performance of the bearings directly affect the operational performance, reliability, and safety of these rotating machines and related systems. Therefore, it is very important to maintain the good condition of the bearings of the rotating machinery. Condition-based maintenance is one of the best ways to maintain the good condition of the machinery which includes the condition monitoring of the machinery and carrying out the maintenance work before it goes to failure. Vibration analysis is the most popular technique for condition monitoring of the bearing. Vibration data collected from the bearing should be analyzed to detect the faults and track the degradation level.

The vibration signal of rolling bearings has a strong non-stationary property which makes it difficult to fault diagnosis. It requires advanced time-frequency signal processing techniques to extract all the relevant information from the vibration signal. All types of signal processing types are studied thoroughly and compared with each other. Finally, Hilbert–Huang transform (HHT) is chosen for analysis of the vibration signals. It has good computation efficiency and does not involve the concept of frequency resolution and time resolution. Empirical mode decomposition (EMD) is the first step of HHT. But, EMD has got a mode mixing problem, which is eliminated by Ensemble empirical mode decomposition (EEMD). So, it is selected as a signal processing technique for this study.

The accelerated run-to-failure vibration data of roller bearings are collected from the RAMS laboratory at NTNU by running the experiments. and each sample is decomposed into a finite number of intrinsic mode functions (IMFs) using the EEMD method. The sensitive IMFs are selected using the correlation coefficient criterion. Five statistical time-domain features and instantaneous energy is extracted from the sensitive IMFs which indicates the condition of the bearings. These features are compared by looking at their three properties: monotonicity, prognosability, and trendability, and the best one is selected as a health indicator of the bearing which can give the current condition as well as tracks the degradation level and the degradation path. The health indicator can be used for the RUL estimation of the bearing and maintenance optimization.

Contents

Preface	i
Acknowledgement	ii
Abstract.....	iii
Contents.....	iv
List of figure and table	vi
List of Figures	vi
List of Tables	vi
Chapter 1 Introduction	1
1.1 Background	1
1.2 Objectives.....	3
1.3 Approach.....	3
1.3.1 Literature study.....	3
1.3.2 Methods.....	4
1.4 Limitations.....	4
1.4.1 Time	4
1.4.2 Student knowledge	4
1.4.3 Availability of experts	4
1.4.4 Corona situation.....	4
1.5 Report Structure	4
Chapter 2 Theoretical background and Literature review	6
2.1 Signal processing.....	6
2.2 Hilbert-Huang Transform	8
2.3 EMD.....	9
2.4 EEMD.....	12
2.5 Hilbert Transform.....	14
2.6 Sensitive IMFs selection Approach	15
2.7 Time-domain features.....	16
2.8 Health indicator Construction.....	16
2.8.1 Monotonicity.....	17
2.8.2 Trendability	17
2.8.3 Prognosability	17
Chapter 3 Case Study.....	19

3.1 Experiment Design	19
3.1.1 Experiment setup	19
3.1.2 Data collection	20
3.1.3 Raw data presentation.....	21
3.2 Data processing.....	23
3.2.1 Data pre-processing	24
3.2.2 Data analysis	24
Chapter 4 Results	32
4.1 IMFs of vibration signal using EEMD.....	32
4.2 Health indicator	33
Chapter 5 Conclusion and Further Work	37
5.1 Summary and conclusion	37
5.2 Discussion.....	38
5.3 Further work	39
Appendix	40
Appendix A.....	40
Appendix B	41
Appendix B	43
Reference	49

List of figure and table

List of Figures

Figure 1: Signal processing and feature extraction.	7
Figure 2: The flow chart of the EMD process.	11
Figure 3: Flow chart of the EEMD process.	13
Figure 4: Experiment setup	20
Figure 5: Vibration waveform for the first sample, Bearing 3.	22
Figure 6: Vibration waveform for the last sample, Bearing 3.	22
Figure 7: Lifetime vibration signal for Bearing 6.	23
Figure 8: Flow chart of the approach for signal processing.	24
Figure 9: Upper envelope and lower envelope	25
Figure 10: IMFs of $x(t)$ using EMD.	26
Figure 11: IMFs of $x(t)$ using EEMD.	27
Figure 12: Hilbert-Huang spectrum of an IMF of the last sample of bearing 7.	28
Figure 13: Normalized sensitive factor of the IMFs.	30
Figure 14: Part of IMFs using EMD.	32
Figure 15: Part of IMFs using EEMD.	33
Figure 16: Prognosability, monotonicity, and trendability of sensitive IMFs of 8 bearings. The color from the left indicates sensitive IMF 1 to sensitive IMF 5, respectively.	34
Figure 17: Degradation paths of the bearings characterized by RMS of the fourth sensitive IMF.	34
Figure 18: Prognosability, monotonicity, and trendability of sensitive IMFs of the last 6 bearings. The color from the left indicates sensitive IMF 1 to sensitive IMF 5, respectively.	35
Figure 19: Degradation paths of the bearings characterized by RMS of the third sensitive IMF.	36

List of Tables

Table 1: Bearing's specifications.	20
Table 2: Overview of collected data.	21
Table 3: Correlation coefficient between each IMF and input signal.	29
Table 4: Statistical time-domain features.	31

Chapter 1

Introduction

1.1 Background

Huge economic loss is not only the consequence of downtime of machines or failure on any component but also increases the probability of occurring accidents, which may result in fatality. So, it is being a vital matter; to find the most appropriate method to prevent the failure of any equipment.

A bearing is one of the important components in rotatory machines and has been widely used in various industries. It has been used in many applications like shaft mountings, to reduce friction as well as facilitate relative motion between the two components, and so on. The bearing plays a critical role in rotational machines; its functionality is directly relevant to the operational performance and consequently the reliability and safety of these machines and relevant systems. The degradation of bearings over time is one of the most common reasons for machine breakdown. If the bearing fault is not detected early, then the unstable shaft movement may damage other equipment as well. So, it is a better option if it can be monitor in real-time and detect the fault bearing occurring further damage to other parts ([Cui et al., 2017](#)). According to the report presented by the IEEE motor reliability working team about the reliability of large motors in industrial and commercial installations, bearing related fault is the most common and frequent one (41%) followed by stator related fault and rotor fault in electric motors ([IEEE Motor Reliability Working Group, 1985](#)). So, it is one of the essential components which requires the early faults recognition and tracking of the degradation process. By tracking the degradation process of a component, it makes possible to recognize the bearing's present condition as well as to predict the future condition, which eventually helps to take a maintenance decision before its actual failure. This strategy is known as condition-based maintenance (CBM) which highly reduces operating costs, increases machine reliability, and increases safety level in a workspace. Therefore, it is being widely used in many industries and highly researched for years ([Jardine et al., 2006](#); [Ayo-Imoru & Cilliers, 2018](#); [Chin et al., 2020](#)).

CBM has three main steps, data acquisition, data processing, and maintenance decision support and it has two main aspects; fault diagnosis and prognosis ([Jardine et al., 2006](#)). Fault diagnosis is a process of identification and classification of bearing faults whereas prognosis is a process of monitoring the present condition of a bearing and estimating remaining useful life (RUL) based on the present condition of the bearing. Among several techniques, the vibration-based technique is the most common and widely used one for bearing diagnostics and prognostics as the vibration signals contain plenty of useful information about the bearing's condition and are easy to collect ([Mathew & Alfredson, 1984](#); [Mechefske, 2005](#)). It is possible to detect and predict the machine condition by analyzing the machine vibration signals. It has been widely researched over the past years ([Tandon & Choudhury, 1999](#);

[Carden & Fanning, 2004](#); [Vishwakarma et al., 2017](#); [KiranKumar et al., 2018](#); [Nithyavathy et al., 2021](#)).

In vibration-based analysis, widely used signal processing techniques are time-domain analysis, frequency domain analysis, and time-frequency analysis. Data processing includes two main steps which are data cleaning and data analysis. Signal processing techniques process available raw data to extract useful information and the process is called features extraction. These extracted features are used for fault diagnosis and RUL estimation, but it is very important to have a quantified relationship between bearing degradation and the extracted features. An effective signal processing technique is necessary for the establishment of quantitative relation between bearing degradation and fault features. The selection of appropriate signal processing techniques depends on the nature of the raw signal ([KiranKumar et al., 2018](#)).

A non-stationary and nonlinear signal cannot be described only in the time domain or in the frequency domain. It requires signal processing techniques in the time-frequency domain. Recently, such techniques have been developed rapidly such as wavelet transform (WT), Hilbert-Huang transform (HHT) and Short-time Fourier transform (STFT). Because of the non-stationary and nonlinear nature of raw vibration data, it is necessary to use time-frequency-based signal processing for vibration analysis of bearing to get better results ([Liu & Han, 2014](#)). These techniques are highly applied to fault diagnosis. It is critical to choose the right signal processing technique to get better insights as different signal processing techniques characterize distinct performance ([Lei, 2016](#)). A huge number of researchers are attracted to the use of the wavelet transform method as it is well explained by theory, but self-adaptation is difficult to achieve in this method ([Xu et al., 2019](#)). To compensate for this drawback of the wavelet transform, [Huang et al. \(1998\)](#) proposed Hilbert-Huang transform (HHT) method. The first step of HHT includes empirical mode decomposition (EMD) which increases the adaptability of signal processing ([Zhang et al., 2021](#)). EMD, the most recent technique is getting popular though there is a lack of mathematical explanation. [Patel and Shakya \(2020\)](#) develops a model with an energy-entropy ratio as a feature for early fault detection using EMD and mentioned that EMD is one of the widely used techniques ([Lei et al., 2013](#); [Rai & Upadhyay, 2016](#)). [Lei et al. \(2013\)](#) has reviewed the huge number of articles on the empirical mode decomposition and ensemble empirical mode decomposition (EEMD) used for fault diagnosis of rotatory machinery. [Sun et al. \(2021\)](#) combines EMD with improved Chebyshev distance to extract features from the experimental data for fault diagnosis and it is proved as effective technique from the result.

According to a preliminary literature review about EMD and EEMD, there is a huge number of articles on EMD and EEMD applied for diagnosis of rotatory machinery only, but few results for health indicator construction, which is used for prognosis purpose. It means that it is difficult to find well-explained research about the prognosis of rotatory machinery using EMD and EEMD. Also, the majority of research articles did not provide criteria for sorting of IMFs which are more sensitive towards the fault of machinery. By identifying sensitive IMFs, it will be possible to identify good health indicator, which ends with an effective and correct model for fault diagnosis and prognosis of the rotatory machinery. Besides, it also decreases the simulation time.

In this study, the core topic is to perform a comparison of EMD and EEMD by applying those techniques for features extraction from the experimental vibration signal collected in the RAMS laboratory at NTNU. Secondly, the extracted features are compared in term of monotonicity, prognosability, and trendability of the features, and health indicator is constructed for prognosis purpose.

1.2 Objectives

The objectives of the thesis are listed as follows.

1. Data collection through experiments
 - a. Design of experiments to see what experiments are needed to get to analyze the impact of factors such as particle size, motor speed, etc.
 - b. Run the required number of experiments to record the signals.
2. Discuss the importance of the selection of appropriate signal processing techniques.
 - a. Investigate the different types of signal processing techniques, especially focus on time-frequency techniques.
 - b. Compare and present the best one for bearings feature extraction.
3. Carry out the case study.
 - a. Pre-processing of the signals collected from the experiments.
 - b. Perform signal processing to extract relevant statistical features to construct a health indicator that is used to model the degradation of the bearing.
4. Discussion of all the findings in this study and possibilities about the future works.

1.3 Approach

There are two actors involving actively in this study except for the student, and they are as follows.

1. NTNU: The master's thesis is carried out as the final part of two years master program, RAMS. Jørn Vatn and Bahareh Tajiani will guide the student throughout the project.
2. RAMS Laboratory: The experiments for the data collection are run in the RAMS laboratory with the help of Bahareh Tajiani and Mr. Viggo Gabriel Borg Pedersen.

1.3.1 Literature study

Literature studies of the relevant topics are to be performed and documented well. The important topics for literature investigation in the project are vibration analysis, signal processing techniques, features extraction, Health indicator construction, and so on. All relevant literature will be obtained through literature searches in NTNU university library, google scholar, and databases such as IEEE, ScienceDirect, Scopus, Engineering village, and so on.

Finally, a literature survey regarding data analysis using MATLAB is done enormously. Programming, analysis, and interpolation with MATLAB are learned with the help of the MATLAB Mathworks manual ([MathWorks, 2021](#)) and report prepared by [Houcque \(2005\)](#). The

main challenges faced during the data analysis are to process the huge number of CSV files and deal with large matrices.

1.3.2 Methods

The most important and common methods to achieve the stated objectives are to do thorough literature reviews and regular discussion with the supervisor, co-supervisor, and colleagues. The regular meeting with the supervisor and co-supervisor is scheduled every Wednesday to update the progress and to get feedback from them.

1.4 Limitations

Some limitations that may affect the project are listed below.

1.4.1 Time

The main limitation of the master's thesis is the time limit. The master's thesis is limited to the time frame of 21 weeks including a week Christmas holiday during the Autumn semester. The weekly load is estimated at 40 hours per week. So, it will limit the findings and validation of the findings during this period.

1.4.2 Student knowledge

The second limitation can be the lack of enough practical and technical knowledge about the required fields for the study. As a result, some tasks may be performed poorly by the student.

1.4.3 Availability of experts

Regular discussion and feedbacks from experts during the thesis are important to perform well. As both supervisor and co-supervisor are busy, it is challenging to get the time when the student wants.

1.4.4 Corona situation

The student is supposed to perform experiments in the laboratory. The access time of the laboratory is limited because of this recent pandemic. It may get affected more or in the worse case, can be temporarily closed in the future if the second outbreak takes place.

1.5 Report Structure

Chapter 1 of the master's thesis includes an overview of the project like background, objectives, limitations, approach, and report structure. The remaining chapters in this thesis will be divided into the following three parts:

1. Theoretical investigation and literature review
2. Case study.
3. Discussions, conclusions, and suggestions for further work.

Chapter 2 includes all the necessary theoretical studies including the literature review on the topics like signal processing, empirical mode decomposition (EMD), ensemble empirical mode decomposition (EEMD), features extraction, health indicator construction, and so on. It will provide the theoretical foundation for the case study.

Chapter 3 explains the case study carried out in this project. It includes all the tasks carried out within the case study with all the steps explained in detail.

Chapter 4 presents the finding and results of the study. The features and a health indicator are constructed from the sensitive IMFs of the vibration signals of the bearings.

Chapter 5 provides broad discussions of the findings and limitations of the study. And finally, it includes an overall conclusion and some suggestions for further work.

Chapter 2

Theoretical background and Literature review

In this chapter, a brief description of signal processing classification is presented followed by a detailed theoretical background of Hilbert-Huang transform, empirical mode decomposition, ensemble empirical decomposition, and health indicator construction. This section shows an overview of the research and literature present in the field and shows the state of art within signal processing techniques for vibration signal analysis. The sources for the literature are NTNU University Library, Google Scholar, Google Books, and databases like ScienceDirect, Scopus, Engineering Village, and IEEE. The keywords used for finding the works of literature are signal processing, vibration analysis, rolling element bearings, empirical mode decomposition, EEMD, diagnosis, and prognosis.

2.1 Signal processing

Signal processing is a process of cleaning raw data and applying available algorithms, methods, or tools for better understanding and interpretation of data. Signal processing analyses the cleaned data to extract useful information for a further diagnostic and prognostic purpose which is known as features. The main objective of signal processing is to extract fault-related information of rotatory machinery and increase the signal-to-noise ratio (SNR) ([Lei et al., 2013](#); [Lei et al., 2014](#)). In the case of vibration signal analysis, signal processing can be divided into three main categories as time-domain ones, frequency-domain ones, and time-frequency-domain ones as shown in Figure 1.

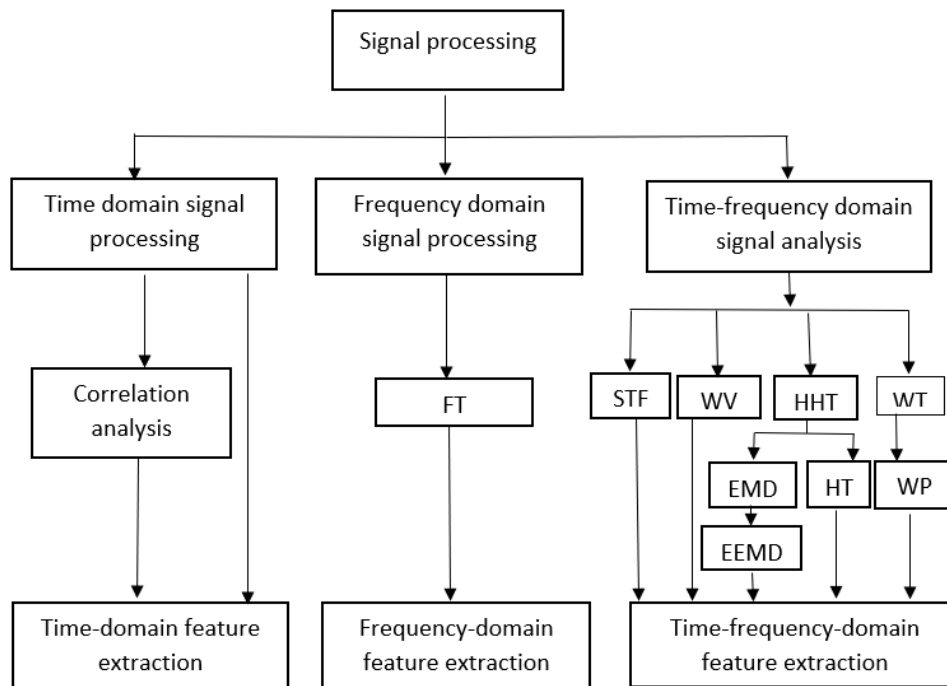


Figure 1: Signal processing and feature extraction (adapted from [Lei \(2016\)](#)).

Time-domain-based signal processing includes correlation analysis and time-domain statistical feature extraction which reflects the statistical properties of a signal. [Motahari-Nezhad and Jafari \(2021\)](#) extracted 60 different statistical features from the acoustic emission (AE) signal of bearing and selected 10 best features using the Improved Distance Evaluation (IDE) method which are used for predicting remaining useful life. [Nayana and Geethanjali \(2017\)](#) propose new time-domain features namely, waveform length (WL), slope sign changes (SSC), simple sign integral (SSI), Wilson amplitude (WAMP) along with traditional features mean absolute value (MAV), and zero-crossing (ZC). He compares the new features with conventional time-domain features like kurtosis, RMS, standard deviation, skewness, and so on and found that proposed time features are better than conventional ones. Only a few recent articles are studying the diagnosis or prognosis of rotatory machinery using only time-domain signal processing. Frequency-domain techniques are denoting to fast Fourier transform (FFT) whose basic functions are a set of trigonometric functions. So, this technique is limited to stationary and linear signals. So, both time domain and frequency domain techniques assume that the signal is stationary and linear which is not the case every time ([Lei et al., 2013](#)). Machinery faults may be non-stationary and non-linear ([Meltzer & Dien, 2004](#); [Cempel & Tabaszewski, 2007](#)). To realize non-stationary signals, several advanced time-frequency analysis techniques have been introduced and applied to fault diagnosis of rotating machinery such as wavelet transform, short-time Fourier transform, Hilbert-Huang transform (HHT), and so on ([Bartelmus & Zimroz, 2009](#); [Urbanek et al., 2012](#)). Short-time Fourier transform provides both time and frequency information, but its performance is affected badly by the Heisenberg uncertainty principle which is solved by the application of the wavelet transform method ([Loughlin et al., 1992](#)). Wavelet transform is one of such methods which is widely used for roller bearings and analyzes the vibration signals using a distribution of energy to time along with each frequency band ([Lou & Loparo, 2004](#); [Junsheng et al., 2005](#); [Xiao et al., 2012](#)). Wavelet transform is taken as one of the effective time-frequency

techniques ([Z. K. Peng et al., 2005](#); [Yong et al., 2011](#)). [Bastami and Bashari \(2020\)](#) develop an effective Spectral kurtosis compared to general spectral kurtosis using wavelet transform. Despite WT is one of the best available ones and widely used for vibration fault diagnosis, it has got some inevitable deficiencies and limitations ([Peng et al., 2002](#)) such as it uses fixed decomposition scales for analysis without considering the signal characteristics and limited length of wavelet function which causes energy leakage ([Z. Peng et al., 2005a](#); [Yu & Junsheng, 2006](#)). Hilbert-Huang transform ([Huang et al., 1999](#); [Montesinos et al., 2003](#)) is a recent popular time-frequency analysis method that has good computational efficiency and does not use fixed decomposition of frequency resolution and time resolution. This technique works through performing a self-adaptive decomposition method named empirical mode decomposition (EMD). The roller bearing signals are often non-stationary and nonlinear which means their frequency components change with time. So, it is not a good idea to realize the bearing vibration signals using time-domain or frequency-domain alone. Considering the limitations of the wavelet transform, EMD can be taken as the best option for signal decomposition for the effective and precise realization of vibration signals.

2.2 Hilbert-Huang Transform

Hilbert-Huang transform is one of the gaining popularity time-frequency analysis methods. It is a combination of two steps; recently developed empirical mode decomposition and well-known Hilbert transform (HT) which is proposed by ([Huang et al., 1998](#); [Huang et al., 1999](#); [Huang & Busalacchi, 2000](#)). In the first step, EMD decomposes the original complicated signal to a finite number of time-varying mono-component functions called intrinsic mode functions (IMFs). [Cohen \(1995\)](#) has introduced a mono-component function as a function that has only one frequency at any given time, therefore it can only represent one component. The IMFs of the signal are arranged with decreasing frequency magnitude. The highest frequency component is always represented by the first IMF. EMD is adaptive and is based on the local characteristics of the signal. So, it is highly efficient and is very useful to extract information from non-stationary and nonlinear signals ([Lei, 2016](#); [Phan & Chen, 2017](#)). In most of the cases studied using EMD provides better results when compared to other classical methods because of its skill in revealing the hidden characteristics in the complicated signals ([Lei et al., 2015](#)).

And the second step is to take Hilbert transform on all IMFs which obtains the instantaneous magnitude and frequency of the IMF to time. This instantaneous frequency reveals the physical meaning of local phase change for IMFs. Because of the combination of EMD and HT, HHT can provide a more physically meaningful time-frequency and energy representation of a signal. This is the reason, HHT has been applied for signal analysis in different fields like mechanical engineering ([Feldman, 2011](#); [Ondra et al., 2021](#)), biomedical ([M.-C. Wu & N. E. Huang, 2009](#)), earthquake engineering ([Yinfeng et al., 2008](#); [Li et al., 2016](#)), structural health monitoring ([Chen et al., 2014](#)), and so on. These applications and the huge number of successful studies have shown that HHT is an effective and promising tool for analyzing non-stationary and nonlinear signals despite not having a rigorous mathematical background.

2.3 EMD

The basic idea of EMD is to decompose the non-stationary and nonlinear time series into a finite set, often a small set of oscillatory modes by using a procedure called the sifting process. [Z. Wu and N. E. Huang \(2009\)](#) have mentioned that the number of IMFs is closely equal to $\log_2(N)$ where N is the total number of data points. These oscillatory modes are termed intrinsic mode functions (IMFs) which are different mono-component signals. The number and selection of IMFs depend on the signal itself rather than other algorithms. So, it is a self-adaptive signal processing technique and perfects for the analysis of non-stationary and nonlinear statistical processes.

[Huang et al. \(1998\)](#) proposed the EMD method for the first time in 1998. The IMFs generated by the shifting process should satisfy two conditions as follow.

1. The number of extremum and the number of zero-crossings must be equal or differ at most by one.
2. At any point, the mean value of the upper envelope defined by the local maxima and the lower envelope defined by the local minima is zero.

The linear sum of the finite number of IMFs and residue which is obtained at the end of the decomposition is the signal itself. The relation of the IMFs, residue, and the signal is shown in

this equality $x(t) = \sum_{i=1}^I c_i + r_i$ where $c_i (i = 1, 2, \dots, I)$ are IMFs and r_i is residue. The residue

of the signal does not carry any information but reflects the trend of the signal. EMD does not involve other time-consuming operations, therefore, HHT can deal with the signal of large size.

The basic algorithm of the EMD process for the input signal $x(t)$ is described in the following steps ([Huang et al., 1998](#)).

1. Identify local maxima and minima of the multi-component signal $x(t)$
2. Interpolate the local maxima and the minima by cubic spline lines to form the upper envelope $e_{\max}(t)$ and lower envelope $e_{\min}(t)$.
3. Calculate the mean of the upper and lower envelopes.

$$m(t) = (e_{\max}(t) + e_{\min}(t)) / 2$$
4. Construct the first proto mode function. $h_1(t) = x(t) - m(t)$
5. The component $h_1(t)$ is considered as the first IMF if it satisfies two basic properties.
 - a. The number of extrema and zero-crossing differs by no more than one.
 - b. It has zero local mean. In practice, the second condition means that the mean is globally smaller than a defined tolerance.
6. If $h_1(t)$ is not IMF, assign $x(t) = h_1(t)$ and iterate all the above steps from 1-5 until the first IMF is found (referred to as a sifting process). [Huang et al. \(1998\)](#) have determined a criterion for stopping the shifting process to stop instead of zero local mean. This is computed by putting a limit to the standard deviation of two consecutive shifting results, for example, h_{k-1} and h_k . Standard deviation is computed as:

$$SD = \sum_{t=1}^T \left[\frac{|h_{k-1}(t) - h_k(t)|^2}{h_{k-1}(t)} \right] \quad (1)$$

A typical value for SD is set between 0.2 and 0.3. If the standard deviation is less than the set criterion, the shifting process is stopped, and the shifting result is one of the IMFs.

7. Once the first IMF $c_1(t)$ is found, assign residue as $r_1(t) = x(t) - c_1(t)$. Check if $r_1(t)$ is a monotonic trend or smaller than a defined tolerance. It is the end of decomposition if it true else if, assign $x(t) = r_1(t)$ and go to step (1) (shifting process).

Consider $r_N(t)$ is the monotonic residue after N IMFs are generated, then the original signal $x(t)$ can be generated by adding all IMFs and the residue $r_N(t)$.

$$x(t) = c_1(t) + c_2(t) + \dots + c_N(t) + r_N(t) \quad (2)$$

The basic flow chart of the EMD process for the input signal $x(t)$ is shown in Figure 2.

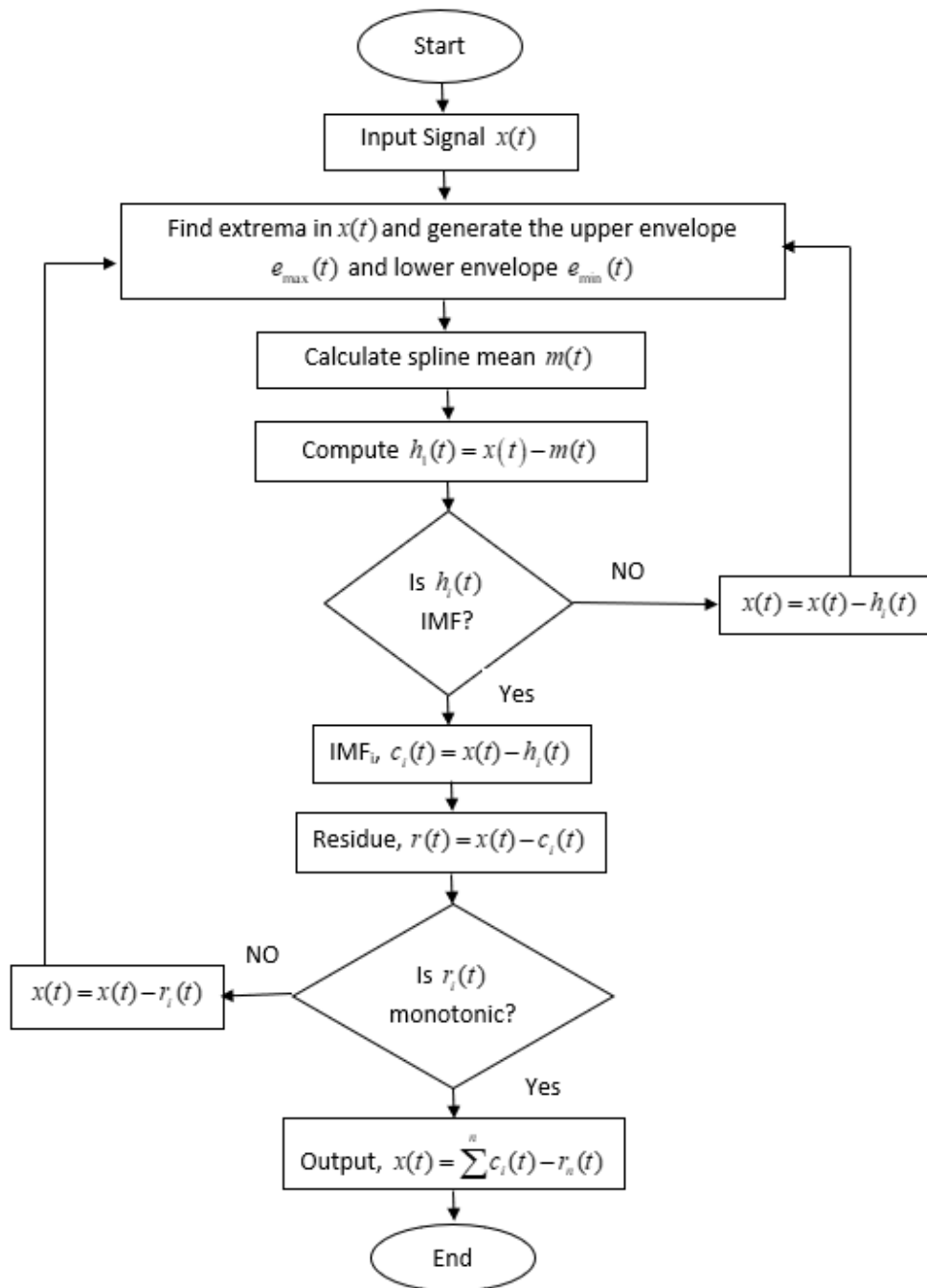


Figure 2: The flow chart of the EMD process.

A detailed explanation of the process of EMD decomposition with examples illustrated can be found in (Huang et al., 1998). After the generation of IMFs from a signal, Hilbert transform can be applied to generate the instantaneous frequency and amplitude of each IMFs.

Despite getting huge popularity and success in the research field, EMD techniques got some drawbacks and deficiencies. In the last few years, several studies complained as it is only an empirical algorithm with a lack of mathematical explanation. Many researchers have suggested different approaches to overcome the drawbacks of EMD such as mode mixing, end effects, shifting process stop criterion, and so on (Rato et al., 2008; Z. Wu & N. E. Huang, 2009). Z. Peng et al. (2005b) compared the correlation coefficients of IMFs with the original

signals. All IMFs with low correlation coefficients are unrelated to the signal, so they are discarded because unrelated IMFs may distort the results. [Lei and Zuo \(2009\)](#) have applied ensemble empirical mode decomposition (EEMD) which overcome the mode mixing drawbacks of EMD. Besides, sensitive IMFs are identified using correlation coefficient for better results. Sensitive IMFs are closely related to health conditions and sensitive to faults of rotatory machinery. Few studies have been reported regarding the lack of orthogonality of IMFs and have proposed some new methods to overcome it ([Lou & Huang, 2007](#)). [Z. Peng et al. \(2005b\)](#) have used wavelet packet transform (WPT) as pre-processing to decompose the signal into a set of narrowband signals before the application of EMD to overcome the problem of orthogonality and achieve truly mono-component IMFs with the decomposition of a signal using EMD.

2.4 EEMD

Mode mixing is one of the major deficiencies of EMD which is eliminated by the application noise-assisted data analysis method termed ensemble empirical mode decomposition (EEMD) which is proposed by [Z. Wu and N. E. Huang \(2009\)](#). It is taken as a valuable aid to EMD ([Colominas et al., 2012](#); [Wang et al., 2016](#)). EEMD decomposes a signal after adding white Gaussian noise to the signal in many trials and the final IMF is taken as the average one. EEMD is based on the statistical properties of the white noises. When white noise is added to a signal, EMD behaves as an effective self-adaptive dyadic filter bank ([Flandrin et al., 2004](#); [Wu & Huang, 2004](#)). The noise-added signal has a continuous distribution throughout the time scale which eliminates interruption and intermittency ([Wang et al., 2019](#)). To enhance the accuracy of HHT for fault diagnosis of rotatory machinery, [Lei and Zuo \(2009\)](#) have proposed an improved HHT which is based on EEMD and sensitive IMFs. All these studies and investigation promotes the importance of EEMD method. Many articles have proved that EEMD removes the mode mixing problem by illustrating examples ([Lei & Zuo, 2009](#); [Yang et al., 2017](#)).

The basic algorithm of the EEMD process for the input signal $x(t)$ is described in the following steps ([Lei & Zuo, 2009](#); [Z. Wu & N. E. Huang, 2009](#)).

1. Initialize the number of trials in the ensemble as M , the amplitude of white noise and the trial number, $m = 1$.
2. Perform the m th trial on the signal added with white noise.
 - a. Generate a white noise with a given amplitude and add it to the input signal $x_m(t) = x(t) + n_m(t)$, where $n_m(t)$ is the m th white noise and $x_m(t)$ is the noise added signal of the m th trials.
 - b. Decompose the noise added signal into N IMFs using EMD as $c_{n,m}(n = 1, 2, \dots, N)$ where $c_{n,m}$ denotes the n th IMF of m th trials.
 - c. If $m < M$, then repeat the above two steps, (a) and (b) with $m = m + 1$. Repeat above two steps until $m = M$ with different white noise series but having the same amplitude each time.
3. Calculate the ensemble mean of the M trials for each IMF.

$$y_n = \frac{1}{M} \sum_{m=1}^M c_{n,m}, \text{ where } n = 1, 2, \dots, N \text{ and } m = 1, 2, \dots, M.$$

4. The ensemble means y_n ($n=1,2,\dots,N$), of the M trials for all N IMFs, are the final IMFs generated by using the EEMD method.

The flow chart of the EEMD process is shown in Figure 3.

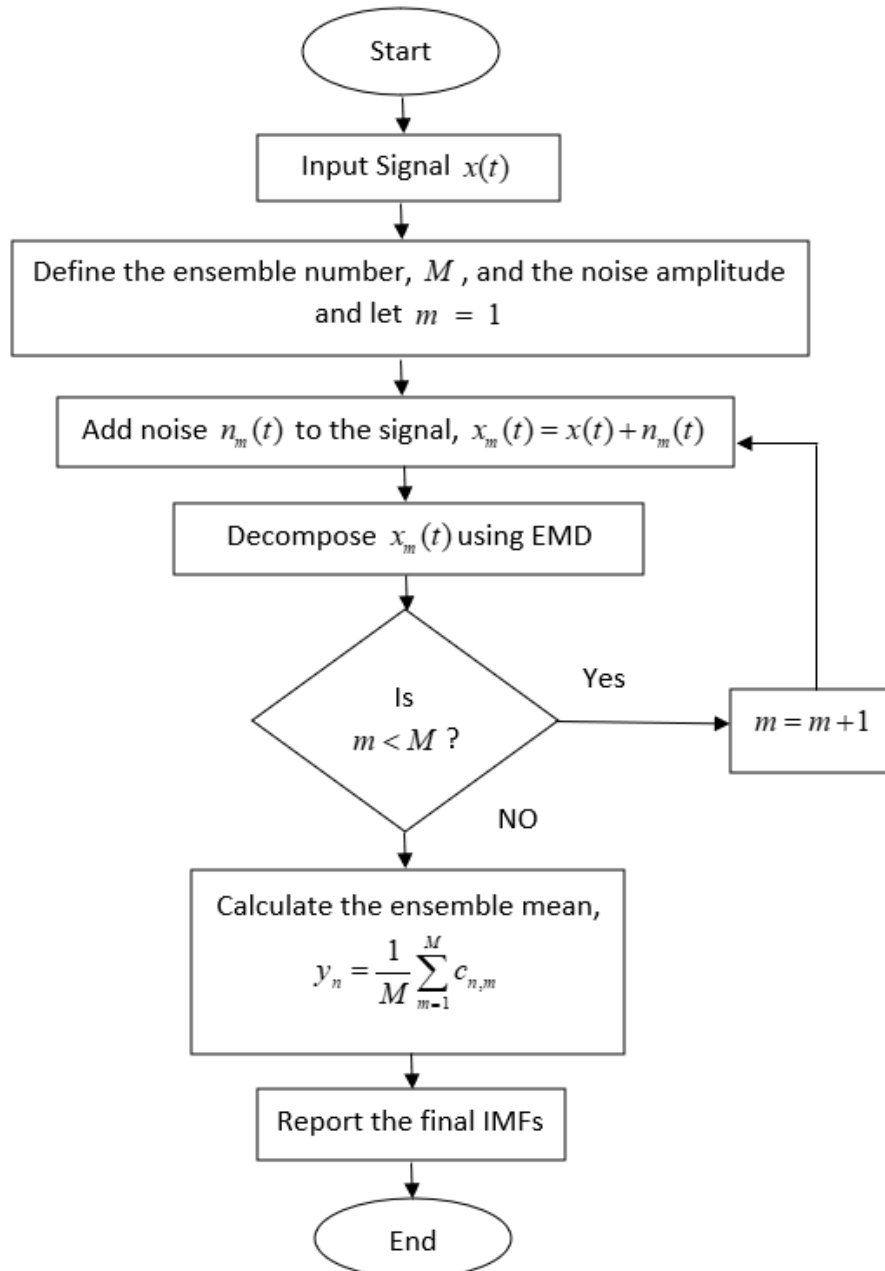


Figure 3: Flow chart of the EEMD process.

The principle of the EEMD methods is illustrated in detail by [Lei et al. \(2011\)](#), and ([Lei & Zuo, 2009](#)). When white noise is added to a signal, the components of the signal automatically set onto proper scales as per the added white noise. As the decomposition is performed after adding different series of white noise in each trial, the result is noisy. But the noise in the result is eliminated or decrease to negligible in the ensemble mean, which is the actual IMF

of the EEMD method. So, the added white noise is just assistance to get better IMFs from the input signal.

The selection of the number of ensembles and amplitude of the white noise is explained by Equation (3) and Equation (4) ([Z. Wu & N. E. Huang, 2009](#)).

$$e = \frac{a}{\sqrt{M}} \quad (3)$$

$$\ln e + \frac{a}{2} \ln M = 0 \quad (4)$$

Where, M is the number of ensembles, a is the amplitude of the white noise and e standard deviation of error whereas error is defined as the difference between the original signal and the corresponding IMFs. [Wang et al. \(2019\)](#) have illustrated with an example for the selection of the number of ensembles and amplitude of the added white noise for the given value of e , normally set as 1%. The study has mentioned one drawback of the EEMD method: computation time consumption of the EEMD. EEMD iterates M times for the decomposition of the input signal using the EMD method which is time-consuming. And the study suggested adding white noise in only one IMF generated from EMD which has the highest kurtosis value and perform the EMD again to select the IMF with the highest frequency as a final IMF. However, the study has supported the EEMD concepts by introducing a white noise in the input signal for the same purpose.

2.5 Hilbert Transform

Hilbert transform is the second step of Hilbert-Huang Transform (HHT). After the IMFs are generated using EMD or EEMD, Hilbert transform (HT) is applied to each IMF to get the full time-frequency-energy distribution of the vibration signal which is called as Hilbert-Huang spectrum.

The Hilbert transform of a signal $x(t)$ is defined as the convolution of signal $x(t)$ and $1/t$. HT can emphasize the local properties of $x(t)$ and defined by the equation.

$$y(t) = H[x(t)] = x(t) * \frac{1}{\pi t} = \frac{\int_{-\infty}^{\infty} \frac{x(\tau)}{t-\tau} d\tau}{\pi} \quad (5)$$

Where the symbol $*$ represents the convolution operation. The analytic signal $z(t)$ can be obtained by combining $y(t)$ and $x(t)$, and it is given as.

$$z(t) = x(t) + jy(t) = a(t) \exp[j\theta(t)] \quad (6)$$

Where $a(t) = \sqrt{x^2(t) + y^2(t)}$ is the instantaneous amplitude of $x(t)$ and $\theta(t) = \arctan\left(\frac{y(t)}{x(t)}\right)$ is the instantaneous phase of the signal, $x(t)$. The instantaneous amplitude reflects the

variation of signal energy with time. The instantaneous frequency is defined simply as shown in Equation 7 as generated IMFs are almost mono-component.

$$w(t) = \frac{d\theta(t)}{dt} \quad (7)$$

Then the Hilbert envelope spectrum is given as follows.

$$h(t, f) = \int_{-\infty}^{\infty} \sqrt{x^2(t) + y^2(t)} \exp(-j2\pi ft) dt \quad (8)$$

So, it is possible to obtain instantaneous frequency from the complicated signal $x(t)$, and it is because of EMD and EEMD which generates almost mono-component IMFs (Lei & Zuo, 2009). Equation 8 enables to represent instantaneous amplitude and instantaneous frequency against time, in a three-dimensional plot in which amplitude is the height of time and frequency plane. The 3D plot is referred to as the Hilbert Huang spectrum.

2.6 Sensitive IMFs selection Approach

All IMFs do not contain useful and relevant information about the decomposed signal. For effective diagnosis or prognosis purpose, those IMFs which do not contain relevant information should be discarded during further analysis. Those IMFs which are closely correlated to the input signal contain useful information related to the health condition and faults of the signal. Hence, it is important to find out the sensitive IMFs for better results.

By looking at the literature studies, a common method to select the sensitive IMFs generated by the EMD method or EEMD method is based on the correlation coefficient between each IMF and the studied signal and correlation coefficient between each IMFs and the normal signal or when the rotating machinery is new (Lei & Zuo, 2009; Qin et al., 2017; Yang et al., 2017). The mentioned three studies have selected the sensitive IMFs of a signal by the calculation of correlation coefficient, but the approaches are a bit different. The algorithm of one of the approaches for the selection of IMFs, which is followed in this study as well is described as follows (Lei & Zuo, 2009).

1. Suppose the vibration signal under study is $x(t)$ and normal vibration signal is $x_{nor}(t)$ and IMFs of the $x(t)$ are supposed to be y_n , where $n = (1, 2, 3, \dots, N)$ and N is number of IMFs using EMD or EEMD.
2. Calculate the correlation coefficient as μ_n between the n^{th} IMF and the signal $x(t)$ where $n = (1, 2, 3, \dots, N)$.
3. Calculate the correlation coefficient as β_n between the n^{th} IMF and the normal signal $x_{nor}(t)$ where $n = (1, 2, 3, \dots, N)$.
4. Define the information related coefficient η_n as $\eta_n = \mu_n - \beta_n$, where $n = (1, 2, 3, \dots, N)$
5. Define and calculate sensitive factor λ_n as $\lambda_n = \frac{\eta_n - \min(\eta)}{\max(\eta) - \min(\eta)}$, where η is the array of information related coefficients collected in step (4) and $n = (1, 2, 3, \dots, N)$.

6. Sort out the sensitive factor λ_n in descending order along with the corresponding IMFs y_n of the signal $x(t)$ as λ'_n and y'_n , where $n = (1, 2, 3, \dots, N)$. $\lambda'_1 \geq \lambda'_2 \geq \dots \lambda'_n \geq \dots \lambda'_N$ is the sorted sensitive factor.
7. Calculate the difference of sensitive factor d_n as $d_n = \lambda'_n - \lambda'_{n-1}$, where $n = (1, 2, 3, \dots, N)$.
8. Compare the calculated differences in step (7) and find the highest d_n and its index n . Then, the first n IMFs in the sorted series of IMFs are the sensitive IMFs.

A simple and clear example is mentioned by [Lei and Zuo \(2009\)](#) to carry out the above approach with the given series of IMFs and a series of sensitive factors.

2.7 Time-domain features

When a fault occurs in rotating machinery, the vibration signal will change accordingly because of the occurrence of an impulse or shock ([Liu et al., 2013](#)). The amplitude and distribution of the vibration signal will change. These changes in vibration signals can be extracted as a feature by statistical time-domain features. These statistical features can be evaluated to find the health condition of the rotating machinery ([Batista et al., 2013](#)). Statistical quantities calculated from the vibration signal can provide approximate information about faults and can be easily calculated ([Patil et al., 2008](#)). [Verma et al. \(2013\)](#) has investigated some time-domain statistical quantities like RMS, crest factor, kurtosis and jerk to develop fault indicator models of gear in a wind turbine.

Some of the common statistical time domain features are listed in Table 4. Generally, a fault in rotating machinery excites the vibration signals and therefore increases the statistical features like mean value, root means square (RMS), and so on. The features like skewness, kurtosis, crest factor, shape factor, and impulse factor can be used to represent the distribution of vibration signal in the time domain. These features are robust for the indication of impulses and shock present in the vibration signals, and they are more sensitive to the variation of operating conditions and good indicators for faults in the early stages. So, different features indicate mechanical health conditions of the machinery from different aspects. Therefore, it is common and important to calculate a huge number of statical time domain features from the vibration signal and compare the features with each other to find an optimal one for effective diagnosis and prognosis of the rotating machinery ([Lei, 2016](#)).

2.8 Health indicator Construction

Health indicator (HI) construction is the most important step for accurate remaining useful life (RUL) of machinery ([Song et al., 2019](#)). A Signal processing technique analyses the input signal to extract different types of features that describe the health condition of the machinery. But not all the extracted features need to express the true condition of the machinery. So, it is necessary to inspect all the features to know, how good the feature is, to track the health condition and degradation of the machinery. The feature that shows the hidden information from the complex data of the machinery and keeps the proper track of health condition and degradation of the machinery is taken as a health indicator for the machinery. The best or optimal feature selected as a health indicator provides the best

predictive power in modeling a set of data to increase the accuracy in fault detection, diagnosis, and prognosis ([Qiu et al., 2020](#)). The construction of a health indicator is performed by comparing three characteristics of the extracted features: monotonicity, prognosability, and trendability, which are briefly explained in the following section.

2.8.1 Monotonicity

Monotonicity expresses the monotonic trend of the feature when the machinery evolves toward failure. It measures the quantitative value of the feature if it changes in a monotonic manner or not, with the degradation of the machinery. The monotonicity of a feature is measured by the average difference of positive and negative derivatives in a range from 0 to 1. If the monotonicity is 1, then the feature is perfectly monotonic and if the value is 0, the feature is nonmonotonic. Monotonicity is calculated as follows ([Qiu et al., 2020](#)).

$$Monotonicity = mean \left(\frac{\# pos \frac{d}{dx} - \# neg \frac{d}{dx}}{n-1} \right) \quad (9)$$

Where, $\# pos$ and $\# neg$ are the number of positive derivatives and negative derivatives respectively and n is the number of data points of a feature.

2.8.2 Trendability

Trendability measures the similarity of the trajectories from normal to failure stage followed by a feature in several run-to-failure datasets. A feature with a high score for trendability, has trajectories with the same underlying shape which optimizes the RUL prediction. It measures in the range from 0 to 1. If the value is close to 1, the feature has good trendability. Trendability is measured as follows ([Tajiani & Vatn, 2021](#)).

$$Trendability = 1 - std \left(\frac{\# pos \frac{d}{dx} + \# pos \frac{d^2}{dx^2}}{n-1} \right) \quad (10)$$

Where, $\# pos \frac{d}{dx}$ is the number of positive first derivatives and $\# pos \frac{d^2}{dx^2}$ is the number of positive second derivatives and n is the number of data points of the feature.

2.8.3 Prognosability

Prognosability measures the variability of a feature at the failure state of a lifetime data based on the trajectories of the feature in different run-to-failure experiments. It is calculated as a variation of feature's values at failure state to the difference of its initial values and failure values and the formula is shown as follows ([Qiu et al., 2020](#)).

$$\text{Prognosability} = \exp\left(-\frac{\text{std}(F_0)}{|\text{mean}(F_0) - \text{mean}(F_f)|}\right) \quad (11)$$

Where, F_0 and F_f are initial and failure values of the feature respectively and prognosability is measured in the range from 0 to 1 and higher the value of prognosability, better the case.

Chapter 3

Case Study

This chapter explains the case study for this master thesis. It includes the design of experiments, data collection and comparison of data processing techniques, and finally data processing for extraction of features and health indicator construction methods.

3.1 Experiment Design

The experiment has been carried out according to an ongoing PhD project which has been carried out by a PhD student, Bahareh Tajiani within the RAMS field. All the planning and design to run the experiments are prepared with collaboration with Bahareh. The required training and knowledge to carry out the experiments such as operating the equipment, safety rules and regulations in the lab, and procedures of collecting and saving samples from a bearing are provided by Bahareh and Mr. Viggo Gabriel Borg Pedersen.

The experiments are carried out in the RAMS laboratory at Norwegian University of Science and Technology (NTNU), Trondheim, Norway. The experimental setup is designed to perform accelerated run-to-failure experiments on two bearings. For this study, only one of the bearings is contaminated by regular adding lubricant which is contaminated by the solid particles termed as Silicium carbide. Two accelerometers are mounted to the tested bearing to record horizontal and vertical vibration data.

The factors that play a role in the degradation of bearings in the experiment are as follows.

1. Speed of motor.
2. Size and density of Silicium carbide in the contaminated lubricant.
3. A magnitude of an external force applied to the bearing.
4. Room temperature.

Initially, it is planned to run experiments with a varying magnitude of factors such as speed of the motor, contaminated lubrication, and force applied to the bearing. But later, the plan is changed to keep all factors unchanged. The speed of the motor is set as 2975 rpm, contaminated lubricant with the same particle size and density, and no external force is added on the bearing. It is planned to run the experiments as many as possible and at the end of the project, it is possible to run eight experiments. The first experiment is carried out with the motor speed equal to 1500 rpm whereas the remaining all experiments are carried out with the motor speed equal to 2975 rpm.

3.1.1 Experiment setup

The experimental setup designed for the vibration data collection is known as “Bently Nevada (system 1) Rotor Kit, model RK4” which is developed at RAMS laboratory at NTNU. The

purpose of the experiment to collect real run-to-failure data from the bearing. The bearing is accelerated for degradation by the regular pouring of contaminated lubricants.

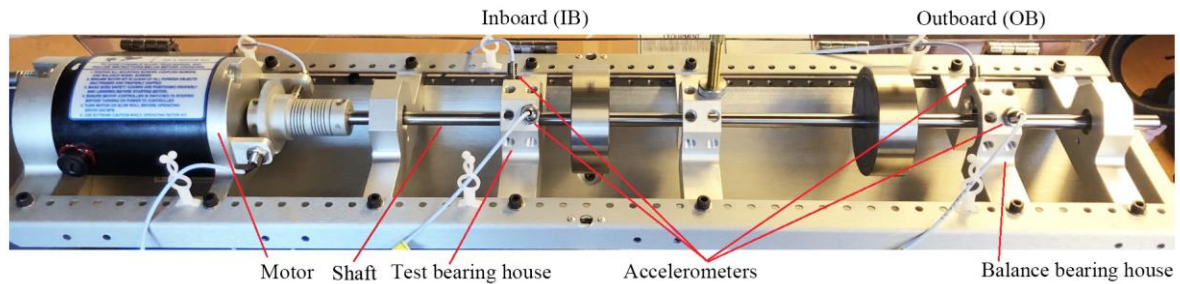


Figure 4: Experiment setup (adopted from [Liu, 2020](#))

The experimental setup is shown in Figure 4. It shows the overview of all the main parts of the setup such as system casing, motor for rotation, shaft, bearings, and accelerometers. The system casing is the main part that holds all the equipment required for the experiments. It holds the motor, two bearing blocks that hold the bearings, holds the shaft and safety cover which is not displayed in the picture. The safety cover is used to close the setup while running the experiments for safety matter. The motor is attached to the shaft which passes through the bearings. The maximum rotation speed for the motor is 1000 rpm.

For the recording of vibration data, two accelerometers are installed in each bearing. One accelerometer is mounted at the top which measures the vertical vibration data and another one is mounted on the horizontal axis which records horizontal vibration data. The recorded vertical and horizontal data should be saved manually.

The specifications of the tested bearings are shown in Table 1.

Table 1: Bearing's specifications ([Tajiani et al., 2020](#)).

Type of Bearing	Open Roller/Ball Bearing
Number of balls	10 balls
Pitch diameter (B), mm	70
Ball diameter, mm	4.7
Inner diameter (d), mm	15.9
Outer diameter (d), mm	34.9

3.1.2 Data collection

In the run-to-failure experiments, horizontal and vertical vibration data are recorded using two accelerometers. Though it is planned to collect data with a different operating condition, later data is collected with the same operating condition as motor speed, time interval to pour the contaminated lubricant, room temperature, and no external force applied to the bearings. The samples of the bearing are saved manually as CSV files every 5 minutes and contaminated lubricant is poured in every 5 samples, which means in every 25 minutes. The

sample collection is continued until the amplitude of vibration reaches the threshold value which is 10g. The threshold value is set as 10g to avoid damage to the motor due to vibration. In each sample, there are 8192 data points and the sample duration is 639.9 milliseconds. The sampling frequency is calculated as $F_s = \frac{8192}{0.64} = 12800\text{hz}$.

Though both horizontal and vertical vibration data are saved on the database, only the horizontal vibration data is used for analysis as vertical vibration data can be affected by gravity ([Tajiani & Vatn, 2021](#)). The overview of the data collected for the study is shown in Table 2. The contaminated lubricant is started to pour after the first 5 samples in the first 2 experiments, but later it is decided to collect 20 samples without adding lubricant to see the normal behaviors of the bearings. So, the contaminated lubricant is poured only after the first 20 samples in the remaining bearings.

Table 2: Overview of collected data.

Bearings	Motor Speed (RPM)	No of Samples Before 10g	No of Normal Samples
Bearing 1	1500	139	5
Bearing 2	2950	146	5
Bearing 3	2950	84	20
Bearing 4	2950	248	20
Bearing 5	2950	152	20
Bearing 6	2950	143	20
Bearing 7	2950	114	20
Bearing 8	2950	123	20

A report proposed by the RAMS laboratory should be filled up every day after an experiment is carried out. It includes information about the experiment that took place. The report is attached in Appendix A.

3.1.3 Raw data presentation

This section presents the raw data to introduce the nature of a single sample and lifetime data of a bearing. Figure 5 and Figure 6 show the vibration waveform of the first sample and the last sample respectively of bearing 3. The first sample has very low amplitude vibration as the bearing is in a healthy state whereas the last sample shows high amplitude vibration (more than 10 g). So, bearing 3 is considered to be in a failure state as the vibration crosses the 10g limit. Figure 7 shows the lifetime waveform of bearing 3 from the healthy state to the failure state. For the first 20 samples, the contaminated lubricant is not added to the bearing, so it shows a smooth graph until $t = 12.8$ seconds (until sample number 20). The lubricant is added after the first 20 samples and after every 5 samples until the amplitude reach till 10g that is the reason the amplitude of the vibration signal starts increasing as the bearing starts getting degraded.

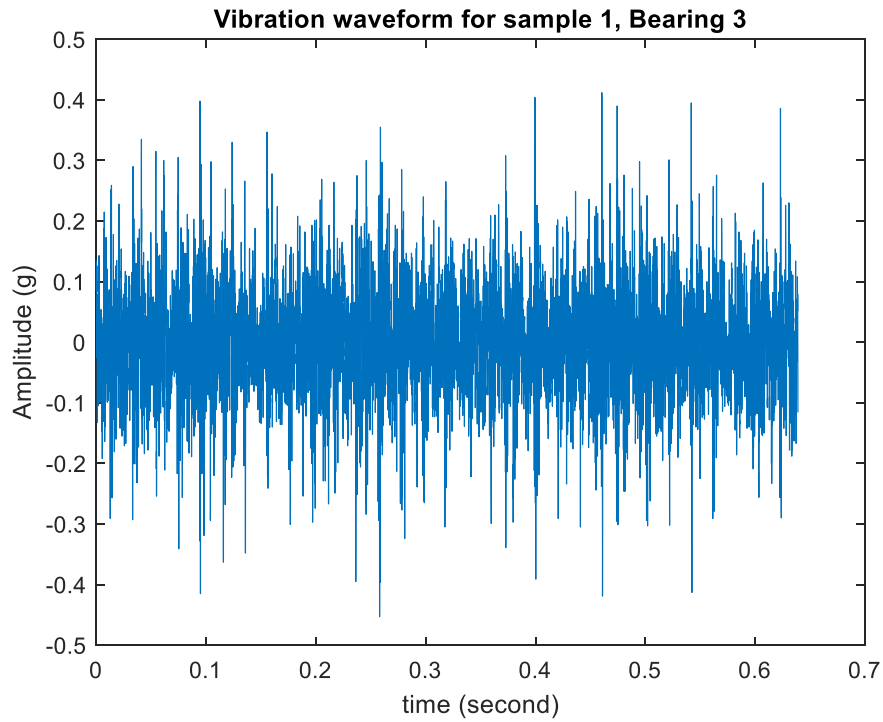


Figure 5: Vibration waveform for the first sample, Bearing 3.

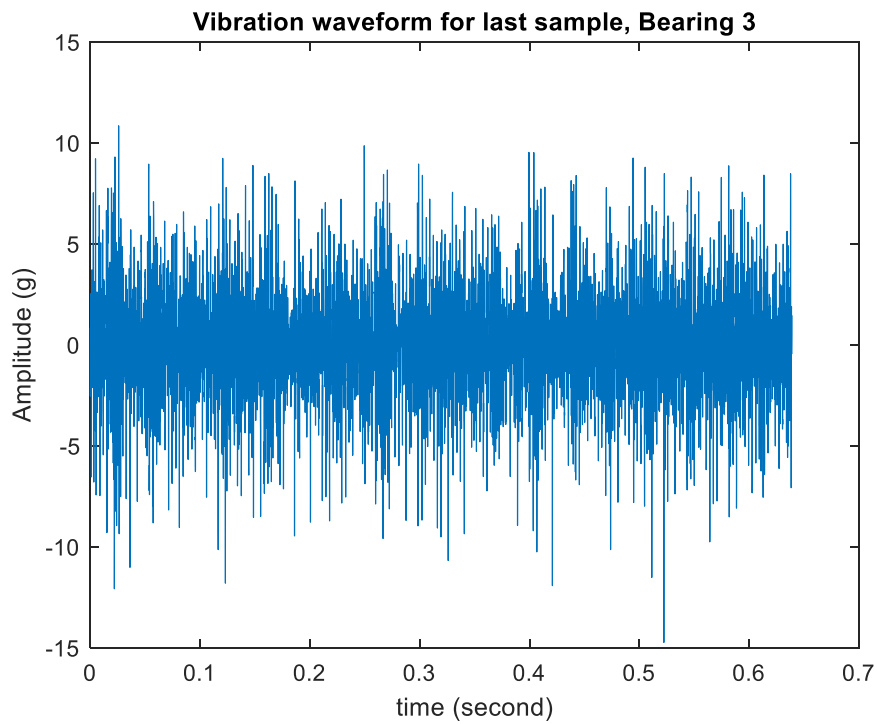
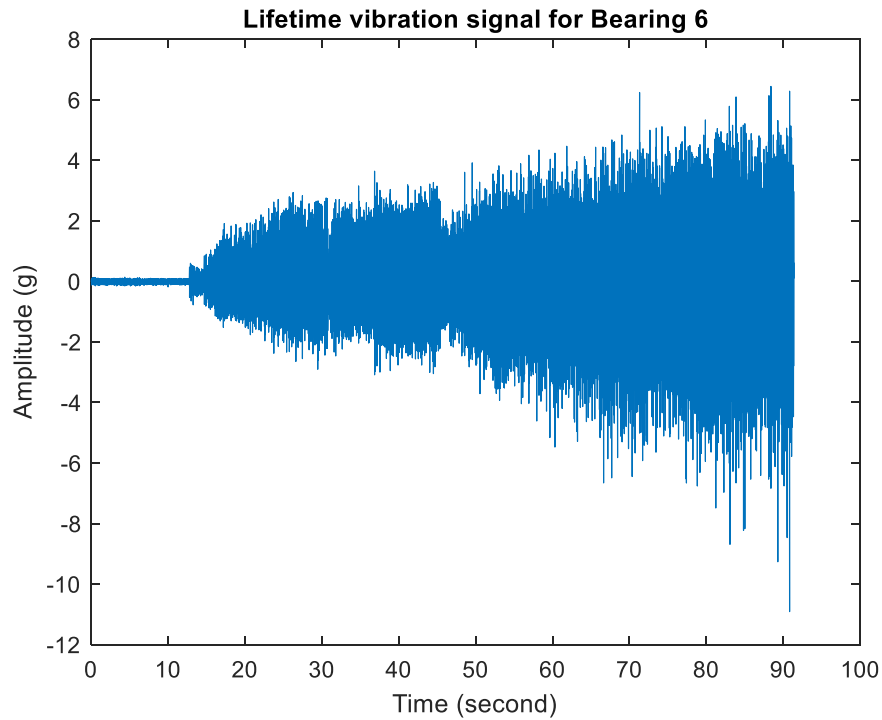


Figure 6: Vibration waveform for the last sample, Bearing 3.



*Figure 7: Lifetime vibration signal for Bearing 6.
(639.9 ms per sample and total 143 samples)*

3.2 Data processing

This section includes the analysis of collected vibration data from the RAMS laboratory for the extraction of useful and hidden information and then compares the characteristics of the extracted features to find the optimal health indicator, which can be used for diagnosis and prognosis of the bearing. The overall approach for data processing is shown in the flow chart as shown in Figure 8. It includes the major tasks performed and all of them are carried out using MATLAB 2020a.

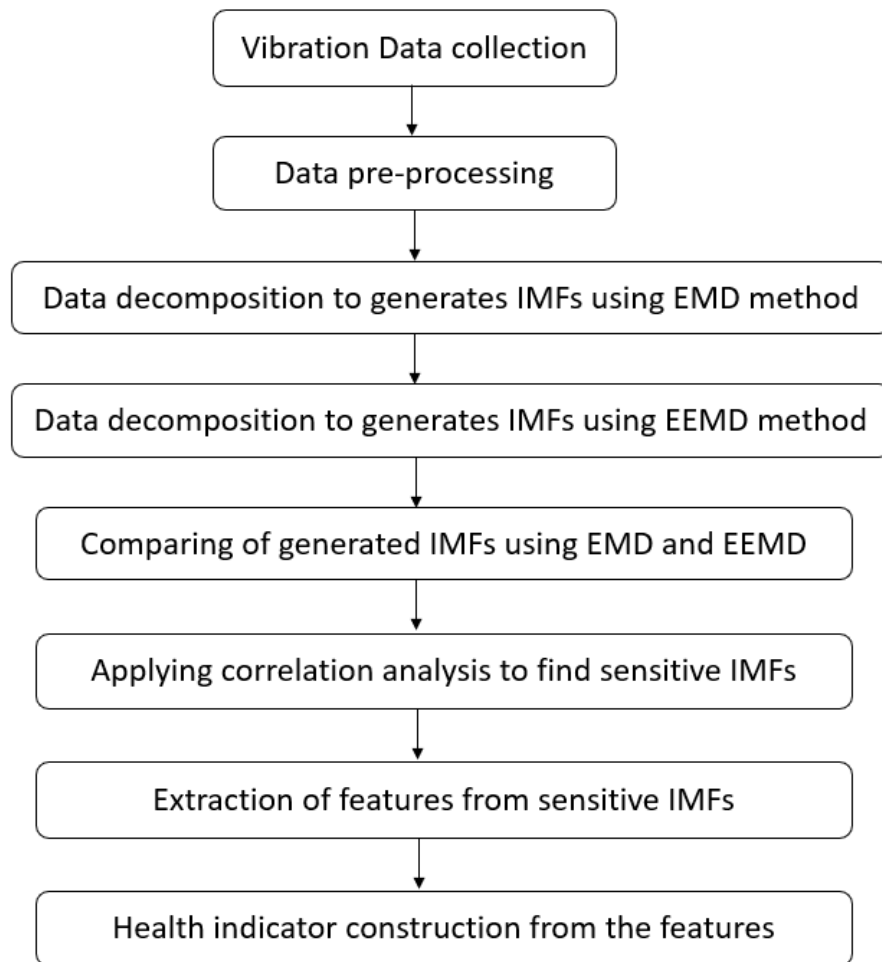


Figure 8: Flow chart of the approach for signal processing

3.2.1 Data pre-processing

Most of the important and useful information in vibration signals collected from rotating machinery is hidden and is embedded in heavy background noise. Therefore, the vibration signal is pre-processed to reduce background noise before performing an actual analysis of the vibration signals.

Mean-centering of the vibration signal is carried out and then data normalization is carried out to change the datasets to a common scale. It helps to get rid of several anomalies that can make the analysis more complicated.

3.2.2 Data analysis

The major task of the data analysis is to decompose the vibration signals into a finite number of IMFs effectively and correctly. For that, two methods are applied which are empirical mode decomposition (EMD) and ensemble empirical mode decomposition (EEMD).

3.2.2.1 Empirical mode decomposition

For the decomposition of a signal, the first challenging task is to find local minima and local maxima and cubic interpolate these extrema. The local minima and local maxima are connected with two cubic splines to form the upper envelope and the lower envelope as shown in Figure 9. For cubic interpolation of the extrema of the vibration signal, a function “spline” of MATLAB is used.

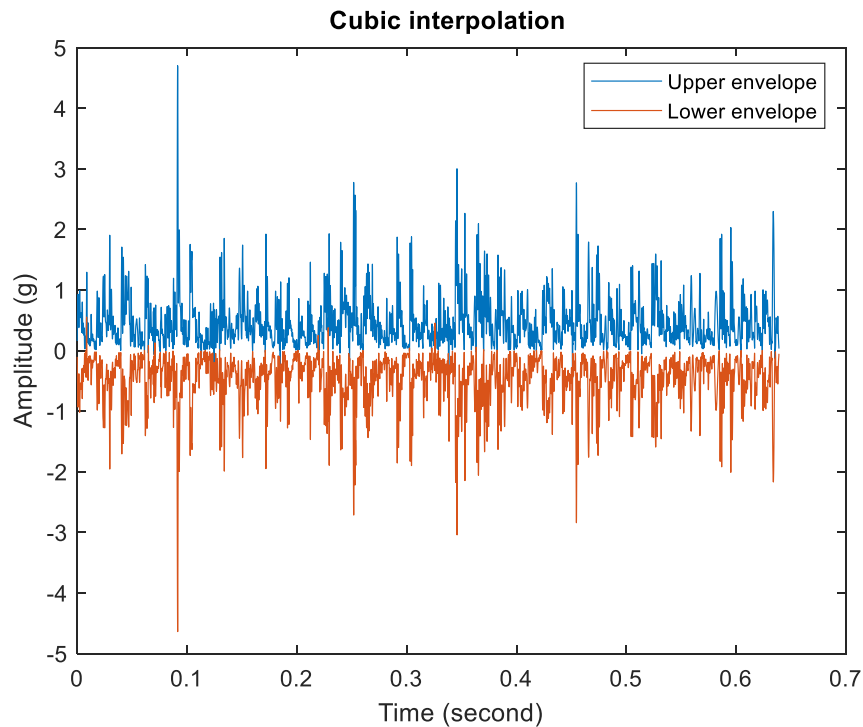


Figure 9: Upper envelope and lower envelope

Vibration samples are decomposed by using the EMD method. The IMFs of the 36th sample of Bearing 8 are shown in Figure 10 including the input signal $x(t)$ and residue. There are 10 IMFs and a residue. All kinds of fault information are contained in these IMFs, which can be identified by extracting a different kind of statistical time-domain features.

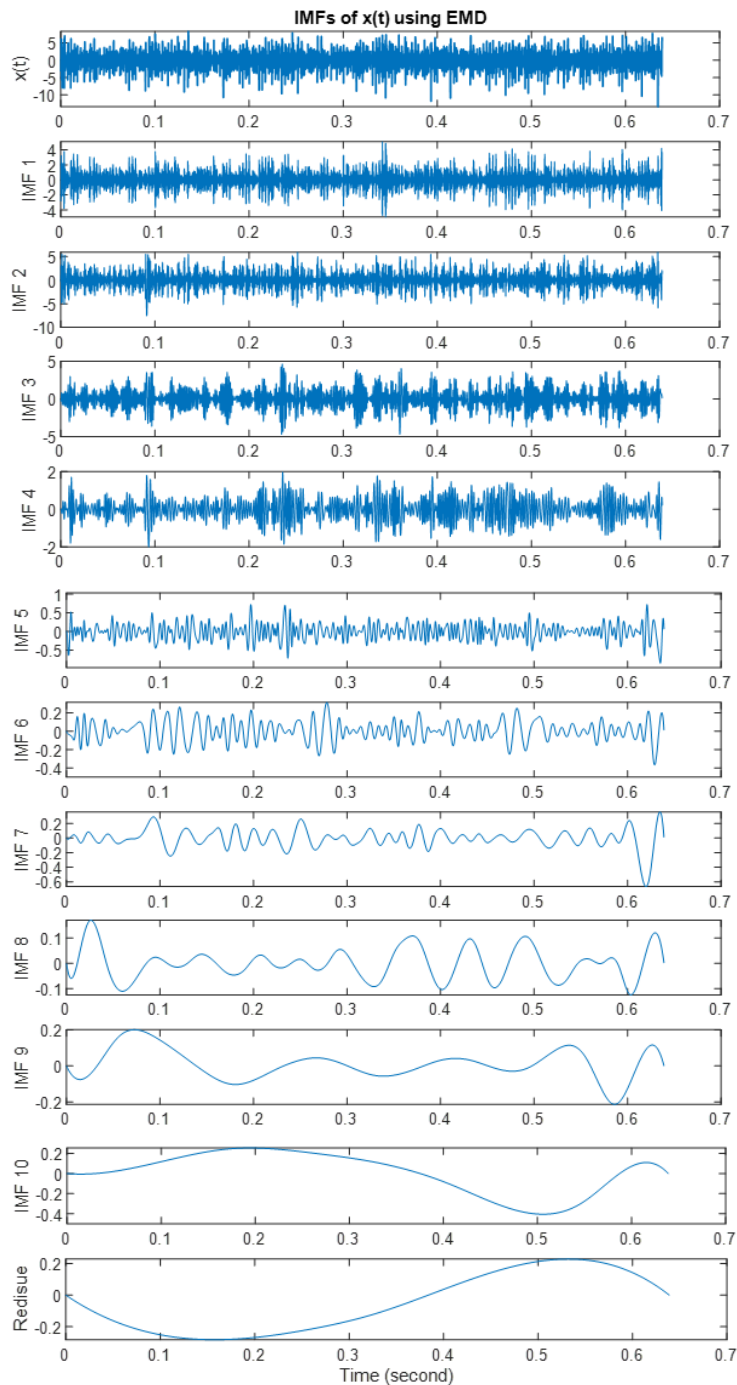


Figure 10: IMFs of $x(t)$ using EMD.

3.2.2.2 Ensemble Empirical mode decomposition

Similarly, vibration data is decomposed into a finite number of IMFs using the ensemble empirical mode decomposition (EEMD) method as well. The challenge in applying the EEMD method is the selection of amplitude of white noise and the number of ensembles. For the selection of the parameters of EEMD, the literature from section 2.4 is followed. Three values for the amplitude of white noise are calculated by setting the error as 1% and the number of ensembles as 100, 200, and 300. The input signal is decomposed three times with three

different amplitudes of noise and selected the best one, which is 200. EEMD is applied to the same signal which is decomposed by EMD in the above section 3.2.2.1. The IMFs generated using EEMD are shown in Figure 11.

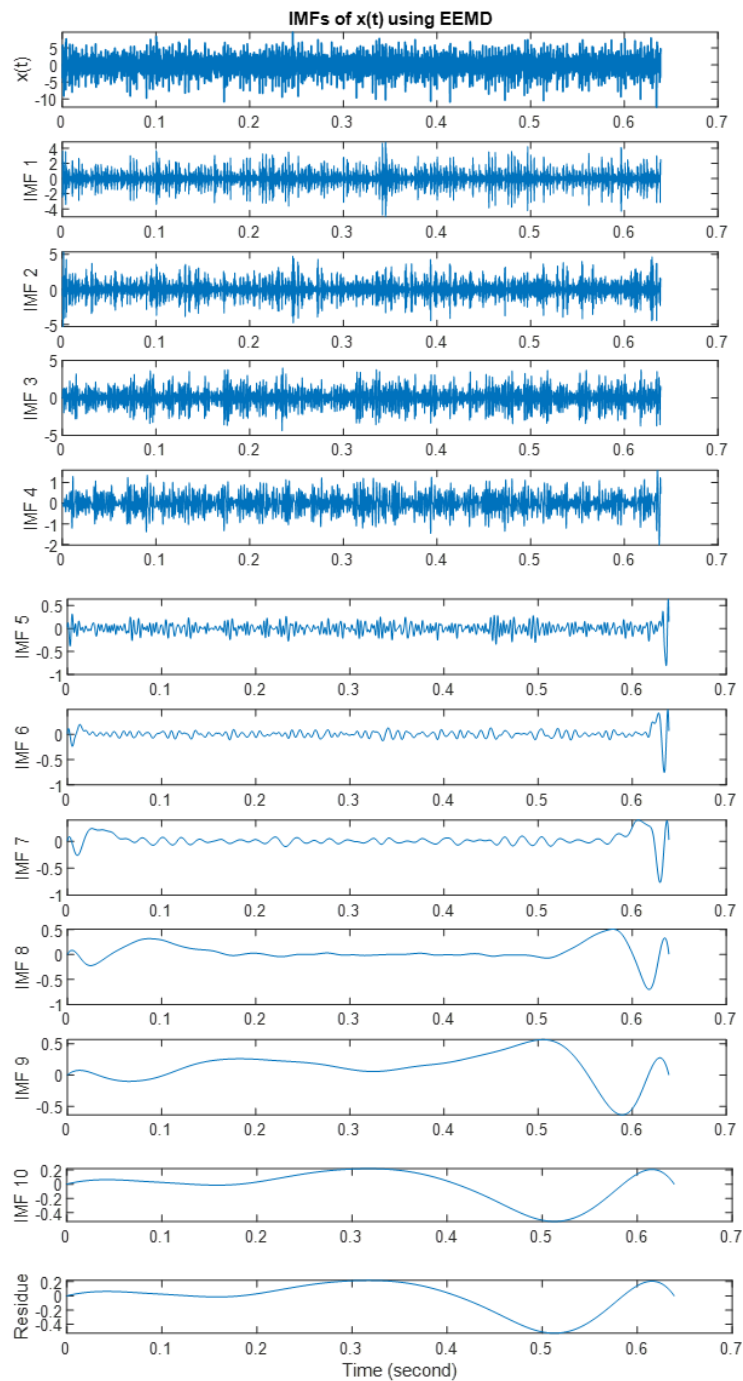


Figure 11: IMFs of $x(t)$ using EEMD.

To alleviate the problem of mode mixing in EMD, ensemble empirical mode decomposition (EEMD) was proposed. To compare the methods, the same vibration sample from bearing 8 is decomposed using both EMD and EEMD methods which are shown in Figure 10 and Figure 11. By looking closely at IMF 5, IMF 6, and IMF 7 decomposed by EMD, two components are present in those three IMFs. And by observing the decomposition result using EEMD, none of

the IMFs contains two components. Thus, EEMD can solve the problem of mode mixing and achieves an improved decomposition with physical meaning. Therefore, the EEMD method is applied for the decomposition purpose in this study.

3.2.2.3 Hilbert-Huang spectrum

The vibration signals are decomposed into a finite number of IMFs and the Hilbert-Huang spectrum can be generated by applying a Hilbert transform to each IMF. The Hilbert-Huang spectrum of the first IMF of the last sample of bearing 7 is shown in Figure 12. The spectrum is a full time-frequency–energy distribution of the vibration signals, which provides a huge amount of information about the faulty frequencies. It is an effective tool for analyzing vibration signals and diagnosis of fault in rotating machinery. The result of the EEMD and Hilbert-Huang spectrum of each IMF are displayed in Appendix B.

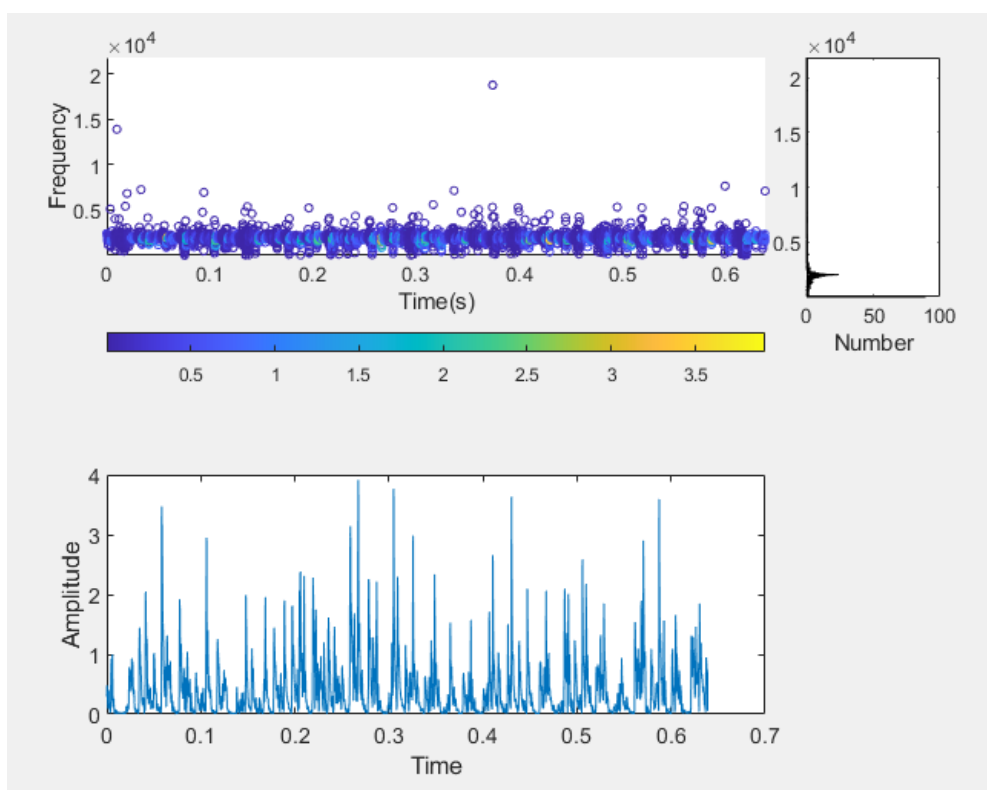


Figure 12: Hilbert-Huang spectrum of an IMF of the last sample of bearing 7.

3.2.2.4 Selection of sensitive IMFs

A finite number of IMFs is obtained after EEMD is performed in the input signal. Some IMFs contain useful information about the health condition of the machine and sensitive to faults of the machine and termed as sensitive IMFs. Therefore, it is beneficial to identify those sensitive IMFs and eliminated other IMFs for better results. Other than sensitive IMFs do not contain information useful for diagnosis and prognosis of the machine.

The approach to select the sensitive or effective IMFs is based on two series of correlation coefficients: the first one is the correlation coefficient between the input signal and its IMFs and the second one is the correlation coefficient between normal signal and the IMFs of the input signal. Two methods for the selection of sensitive IMFs are performed. According to the

first method, those IMFs which has a higher correlation coefficient between the input signal and its IMFs (higher than 0.1) are selected as sensitive IMFs (Qin et al., 2017). The second method follows the steps explained in section 2.6. The example of the calculated correlation coefficient and their normalized values are shown in Table 3.

Table 3: Correlation coefficient between each IMF and input signal.

IMF	IMF 1	IMF 2	IMF 3	IMF 4	IMF 5	IMF 6	IMF 7	IMF 8	IMF 9	IMF 10	IMF 11
Correlation coefficient	0.48	0.634	0.71	0.36	0.07	0.01	0.05	-0.01	0.012	-0.006	-0.01
Normalised correlation coefficient	0.68	0.89	1	0.51	-0.11	0.03	0.08	0.0009	0.03	0.007	0

According to the first method, the first four IMFs are the sensitive ones as they have a high correlation coefficient that is higher than 0.1.

For the second method, the correlation coefficients of all IMFs are normalized to the range from 0 to 1 and sorted in descending order. The difference of sensitive factors is calculated from each adjacent IMFs to find the highest difference. The normalized and ordered sensitive factors are plotted in a graph as shown in Figure 13. It is easily visible that the highest difference is between IMF 4 and IMF 5. So, the sensitive IMFs are IMF 3, IMF 2, IMF 1, and IMF 4 which are the first four IMFs according to the second method.

Results from both methods get matched, therefore the first four IMFs are considered as the sensitive IMFs for the bearing being studied. The same sensitive analyses are performed for all the bearing, and the results varied from the first four IMFs to the first five IMFs as the sensitive IMFs.

Hence, it is decided to consider the first five IMFs as the sensitive ones for all the tested bearings. The statistical features and instantaneous energy are calculated from the sensitive IMFs for further analysis which are discussed in section 3.2.2.5 and section 3.2.2.6.

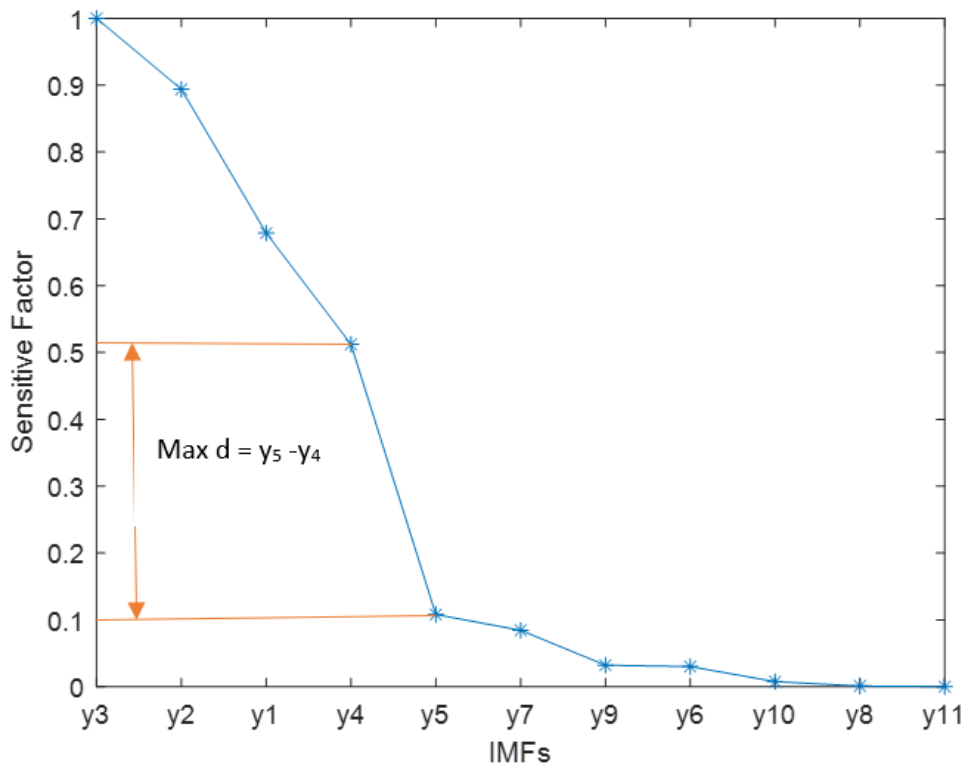


Figure 13: Normalized sensitive factor of the IMFs.

3.2.2.5 Feature extraction

More relevant information of the decomposed vibration signal can be extracted by evaluating the selected sensitive IMFs. The sensitive IMFs contain almost all valid fault information related to the vibration signals of the tested bearing. So, time-domain statistical features and instantaneous energy of IMFs are calculated for comparison. There are five sensitive IMFs of each vibration sample for all the studied bearings and from each sensitive IMF, six features are extracted. The time-domain statistical parameters that are extracted in this study are shown in Table 4 with their formula.

Table 4: Statistical time-domain features ([Tahir et al., 2017](#)).

SN	Features	Formula
1	Kurtosis	$\frac{\sum_{i=1}^N (x_i - m)^4}{(N-1)\sigma^4}$
2	Root mean square (RMS)	$\sqrt{\frac{1}{N} \sum_{i=1}^N x_i^2}$
3	Impulse Factor	$\frac{\max x_i }{\frac{1}{n} \sum_{i=1}^N x_i }$
4	Shape Factor	$\frac{RMS}{\frac{1}{n} \sum_{i=1}^N x_i }$
5	Crest Factor	$\frac{\max x_i }{RMS}$

Besides, time-domain statistical parameter, the instantaneous energy of each IMF is also calculated. The change in the instantaneous energy of IMFs is characterized by the bearing faults, so it can be a feature as a health indicator. The instantaneous energy of each frequency band is calculated by explained by [Loutridis \(2006\)](#).

The instantaneous energy of the sensitive IMFs is calculated as follows.

$$E_i = \frac{1}{2} a_i^2(t) \quad (12)$$

Where, $a(t)$ is the instantaneous amplitude of i^{th} sensitive IMF, $i=1,2,\dots,5$ the number of sensitive IMFs. The instantaneous amplitude is calculated as $a(t) = \sqrt{x_i^2(t) + y_i^2(t)}$, where $x_i(t)$ is i^{th} sensitive IMF and $y_i(t)$ is the Hilbert transform of $x_i(t)$. Hence, Hilbert transform is applied to each sensitive IMF to calculate the instantaneous energy.

3.2.2.6 Health Indicator construction

There are six features extracted from each sensitive IMFs of the vibration samples of the bearings. Among six features, one feature is chosen as a health indicator for the bearings. So, this task is very important and sensitive for further analysis. For the selection of the health indicator, three properties of the features: monotonicity, prognosability, and trendability are compared. The feature is selected as the health indicator which has the highest overall scores for all three measures.

Chapter 4

Results

This chapter includes the key finding of all the tasks performed in the projects. It presents the decomposition of the vibration samples of the bearings using EEMD, presentation of the extracted features from the sensitive IMFs, and finally evaluation of the extracted features to find an optimal health indicator of the bearing.

4.1 IMFs of vibration signal using EEMD

The vibration signal is decomposed into a finite number of intrinsic mode functions which are assumed to be almost a mono-component function. The main objective of EEMD over EMD is that EEMD eliminates the mode mixing problem of the EMD. The problem of mode mixing is visible in IMF 6 generated by using EMD shown in Figure 14 whereas it is not a case on the IMFs generated by using EEMD as shown in Figure 15.

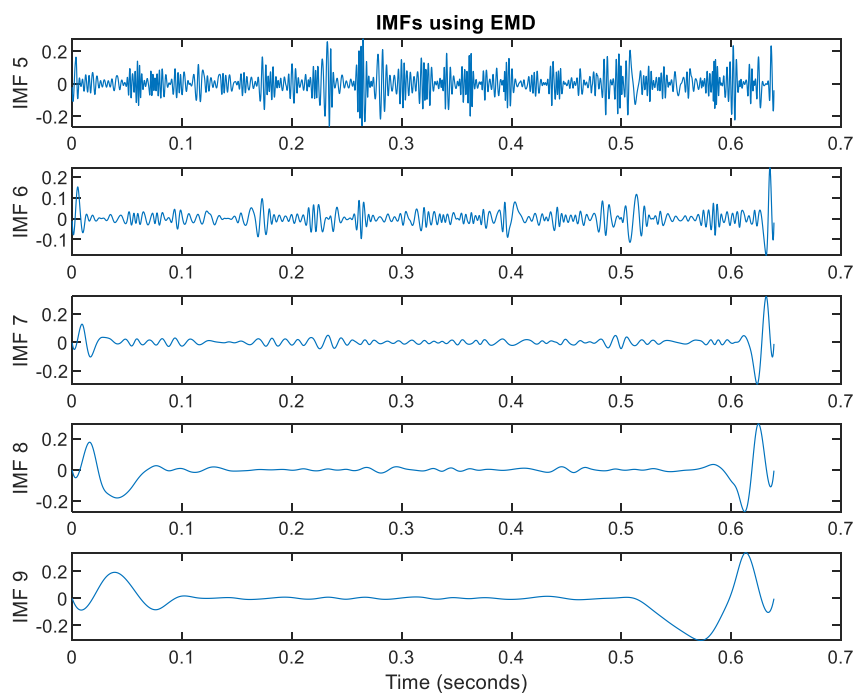


Figure 14: Part of IMFs using EMD.

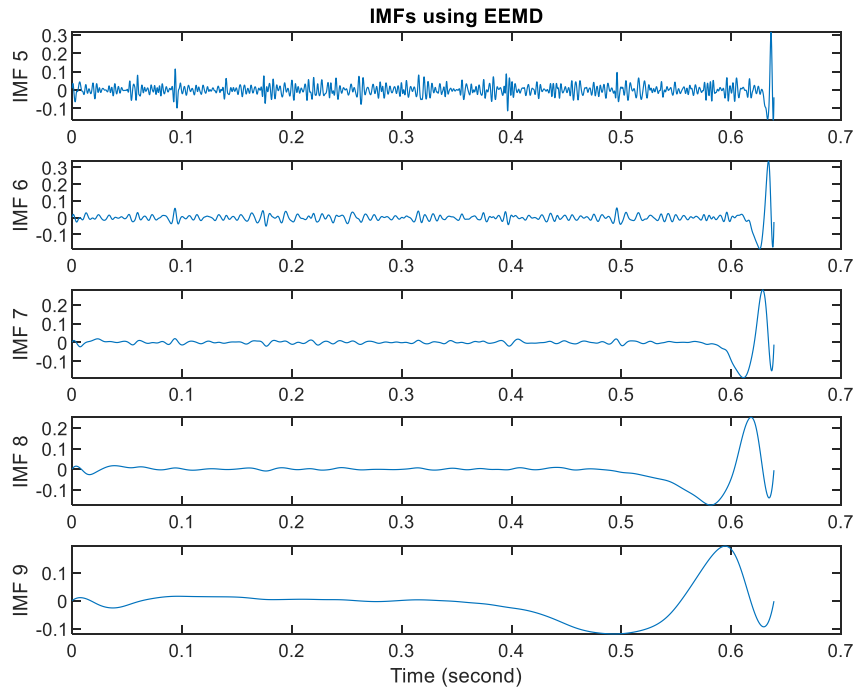


Figure 15: Part of IMFs using EEMD.

An example of the decomposition of a vibration signal into the number of IMFs using EEMD is shown in Figure 11.

4.2 Health indicator

The five time-domain statistical features listed in Table 4 and instantaneous energy are extracted from each sensitive IMFs from the vibration signals of the bearings (bearing 1 to bearing 8). The extracted features are realized and compared in terms of monotonicity, prognosability and trendability and the result is shown in Figure 16. By looking at the three properties of the features, prognosability seems to be almost equal to all the features. In the case of monotonicity and trendability. Instantaneous energy and RMS dominant the other features, but none of the features shows a good score for the trendability. The highest score of trendability is for the fourth sensitive IMF of RMS which is less than 0.4. Among the features, the RMS of the fourth sensitive IMF of the bearings can be taken as the optimal health indicator as it has the highest score for all three measures. The trajectories of the lifetime distribution of RMS for the fourth sensitive IMF of the bearings under study are shown in Figure 17.

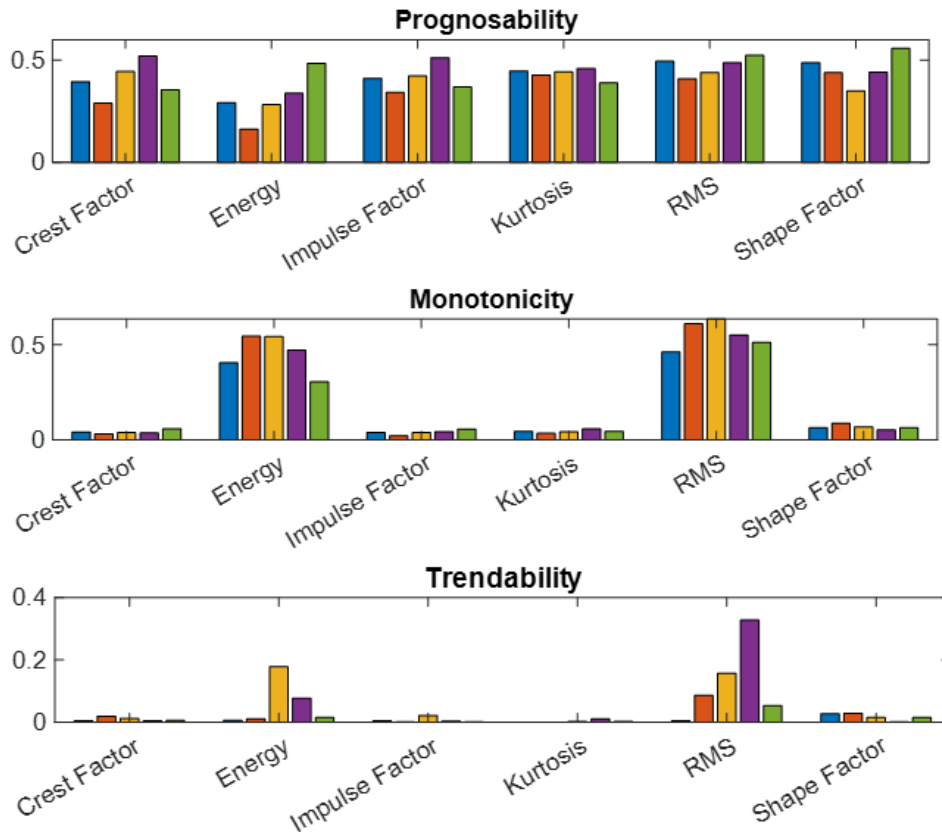


Figure 16: Prognosability, monotonicity, and trendability of sensitive IMFs of 8 bearings. The color from the left indicates sensitive IMF 1 to sensitive IMF 5, respectively.

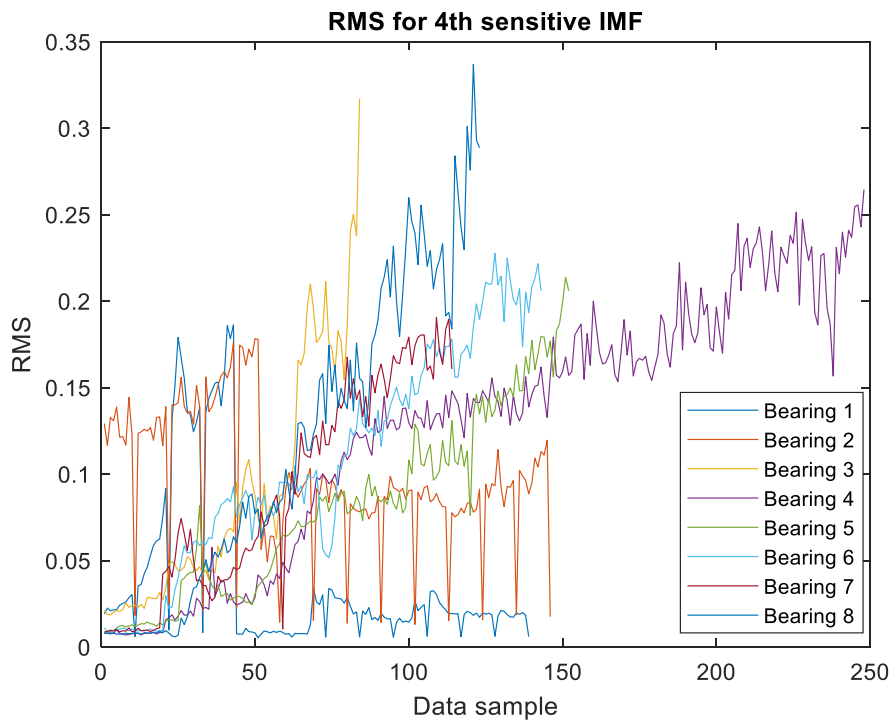


Figure 17: Degradation paths of the bearings characterized by RMS of the fourth sensitive IMF.

From Figure 17, it is visible that RMS values of the vibration samples of bearing 1 and bearing 2 are changing strangely. The value of RMS is fluctuating a lot and shows a sudden decrease at the sample number around 48 and then maintain an almost horizontal path whereas the RMS values of remaining bearings show the gradual increasing path.

The same realization is performed among the vibration samples of the last six bearings after removing the first two bearings to see the variation of the results. The monotonicity, prognosability, and trendability of the features are extracted from these six datasets are shown in Figure 18.

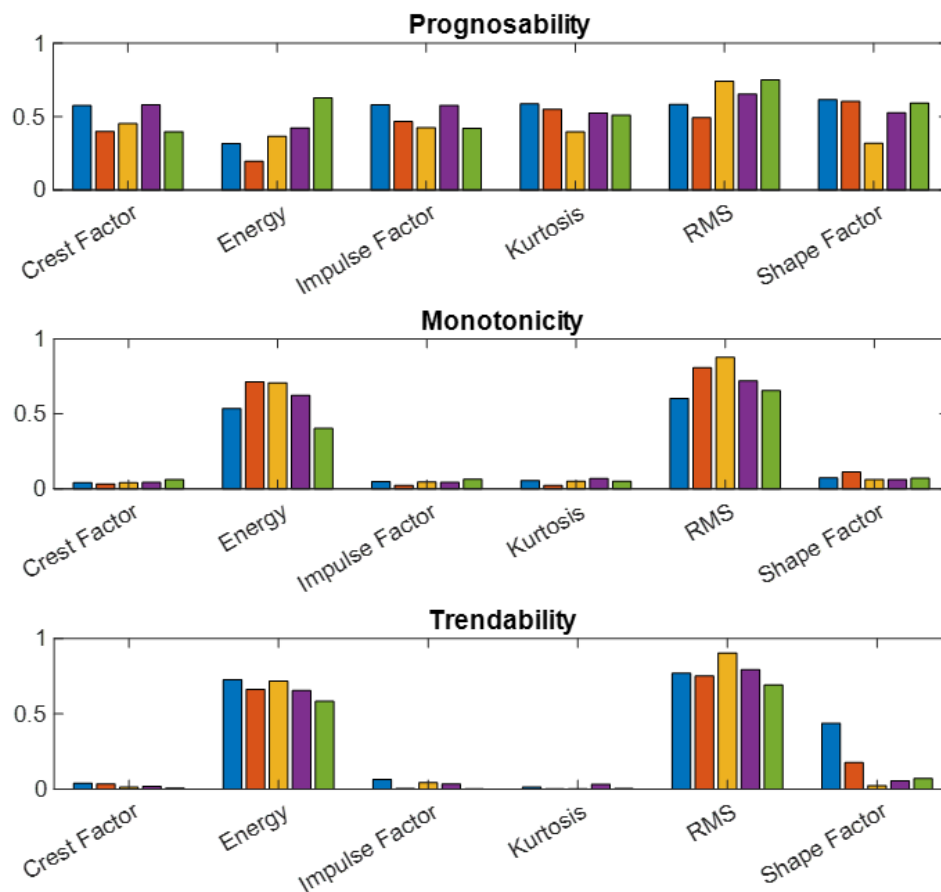


Figure 18: Prognosability, monotonicity, and trendability of sensitive IMFs of the last 6 bearings. The color from the left indicates sensitive IMF 1 to sensitive IMF 5, respectively.

The monotonicity and trendability of RMS, in this case, are improved significantly compared to the earlier case. The comparison can be done by looking at Figure 16 and Figure 18. Looking at the result in Figure 18, RMS and instantaneous energy have dominant all other features. Comparing between RMS and instantaneous energy, RMS for 3rd sensitive IMF has the highest overall score as per the values of monotonicity, prognosability, and trendability.

The degradation paths of the bearings described by the RMS values for the third sensitive IMFs are shown in Figure 19. RMS for the third sensitive IMF has shown good scores for all the properties; monotonicity, prognosability, and trendability, which are required to be a good health indicator. Hence, the RMS of the third sensitive IMFs can be considered as the

optimal health indicator for the bearings. The optimal health indicator is used for modeling the degradation of the bearings and for the estimation of RUL.

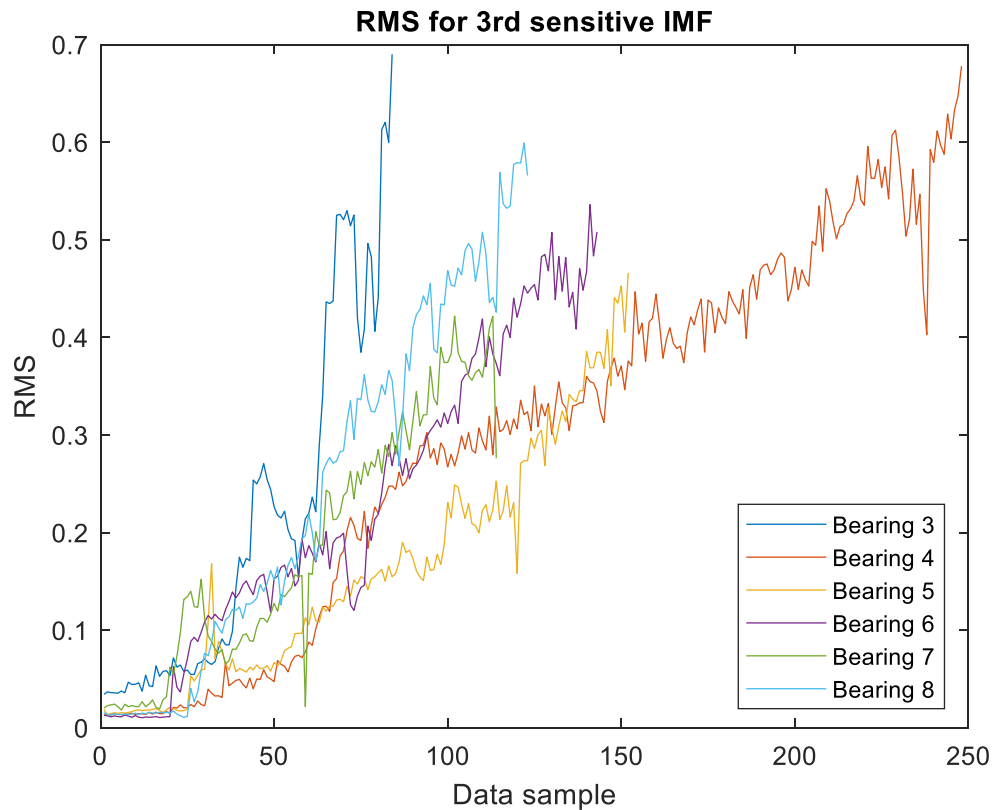


Figure 19: Degradation paths of the bearings characterized by RMS of the third sensitive IMF.

The trajectories followed by the RMS for the third sensitive IMF of the bearing 5, bearing 6, bearing 7, and bearing 8 are close and similar. Also, the time taken by the bearings to reach the failure threshold (10 g) is close to each other, from 114 samples to 152 samples whereas the previous range is 84 samples to 248 samples if the last six bearings are taken into account. This comparison shows that the data collected are getting better and more realistic. So, if more experiments are run, then it will be possible to get the quantitative relation between the degradation of bearing and the optimal extracted feature which helps to give a precise solution for diagnosis and prognosis of the bearings. The degradation paths of bearing 5, bearing 6, bearing 7, and bearing 8 characterized by the RMS of the third sensitive IMF are displayed in Appendix C.

Chapter 5

Conclusion and Further Work

This chapter presents the important discussions about all the tasks done in this project and concludes the study. And at last, it presents some possible recommendations for possibilities and works in future.

5.1 Summary and conclusion

Much research in the field of diagnosis and prognosis of machinery is focusing on selecting the most appropriate and advanced signal processing techniques for developing models and algorithms as precise and accurate as possible. The study carried out as the master thesis has the primary objective to investigate the currently popular signal processing techniques and choose one of the most appropriate techniques for the construction of a health indicator from the vibration samples of the bearings. The tasks performed in this study to fulfill the objectives of the study are discussed in this section.

First, a lot of literature studies are performed to have insight into state-of-art of the signal processing and become familiar with all the required theoretical knowledge for the study. The main topics that are focused to explore are time-frequency-based signal processing, Hilbert-Huang transform, empirical mode decomposition, ensemble empirical mode decomposition, feature extraction, and construction of a health indicator.

The vibration data required for the analysis in this project are collected in the RAMS laboratory. So, the vibration data used to generate the condition monitoring indicator to model the degradation of the bearings are the real data. Eight data sets are collected for the study by running eight experiments. The time required (number of samples) to reach the pre-defined vibration threshold is varying in a large range as illustrated in Table 2, though the bearings type is the same. One of the reasons behind this can be the uncertainties of the experiments as follows.

1. Motor speed: Motor speed is adjusted to a constant value by using a speed control kit, but it is difficult to maintain the constant speed throughout the experiments. The speed of the motor keeps fluctuating throughout the experiment.
2. Amount of contamination in lubricant: Silicium carbide is used to contaminate the oil lubricant which accelerates the degradation of the tested bearings. But, the amount of added lubricant to the bearing is not guaranteed to be constant as it is done manually. The punching vessel used in the experiment to pour the lubricant in the rotating bearing does not pour an equal amount all the time. Besides, the silicium carbide is not equally distributed in the lubricant, it may get settled down in the bottom. Regular shaking of the vessel of the lubricant is required. For, accurate pouring, the process should be carried out automatically within the data collecting system.

3. Sample collection interval: A vibration sample is collected every 5 minutes. As it is done manually, the samples are not collected at the exact timing. So, it should be taken automatically from the system.
4. Looseness of the experimental setup. Sometimes the connection in the experimental setup may get loosen which may affect the reading of vibration samples from the bearings or increase the vibration. During the project, it was experienced in one of the experiments which led to cross the vibration threshold so early. So, the experiment is discarded in the study.

Secondly, an intensive study about the MATLAB functions and methods are studied to program the algorithms for two methods of decomposition of the vibration signals: EMD and EEMD. The coding and testing for the MATLAB program are some of the time-consuming parts of the study. Programming debugging and testing to obtain the intended results are the challenging parts. The algorithm is programmed to generate the series of intrinsic mode functions using both EMD and EEMD methods. The IMFs generated are pretty good as explained in the literature. A comparative study is performed between EMD and EEMD by comparing the IMFs generated by two methods. The results of signal decompositions have explained that EEMD eliminates the mode mixing which is one of the drawbacks of EMD. It shows that EEMD decomposes a vibration signal to the finite number of true IMFs as the mean of an ensemble of trials.

At last, the features are extracted from the collected real vibration data. There is a total of six features extracted from the experimental data, five statistical time-domain features, and the instantaneous energy of the IMFs. The extracted features are evaluated by calculating the monotonicity, prognosability, and trendability of the features and one of the features with the overall maximum scores for all the measures is selected as the optimal health indicator which can be used for the continuous health monitoring and to develop degradation model of the bearings.

Hence, almost all objectives of the project are achieved. It was planned to model a degradation model using the selected health indicator to predict the remaining useful life (RUL) of the bearing if there is enough time. This objective is not obtained because of a lack of time in the project. But, the finding of the project provides a good framework and starting point for the modeling of the degradation model of the bearings. However, further research work is vital for the improvement in health indicator construction, which are discussed in the following section.

5.2 Discussion

The decomposition of the vibration signals following the EEMD process is proved to generate true IMFs of the signal. All the IMFs are almost mono-component. Two methods using correlation coefficient are applied for the selection of the sensitive IMFs. By the combined study of the outcomes of two methods, the first five IMFs are considered as the sensitive or effective IMFs of the vibration signals of the bearings.

The health indicator is developed from the data sets of 8 bearings as the RMS of the fourth sensitive IMF of the vibration signal. The health indicator does not show the good scores of monotonicity, prognosability, and trendability, especially the score of trendability is very low

as shown in Figure 16. So, it is not a good idea to use the selected health indicator for further analysis, for example, for modeling the degradation of the bearing or RUL estimation. By looking at the degradation paths of RMS for the fourth sensitive IMF from all the datasets which are displayed in Figure 17, the first two datasets seem to follow the abnormal degradation paths. These are the very first two data sets collected from the laboratory by the student alone. And hence maybe those data are collected in a wrong way because of the lack of enough experience in running experiments.

So, the results of the same analysis performed on the remaining six data sets after removing the first two data sets are shown in Figure 18 and Figure 19 which are far better. The optimal feature is changed from RMS of the fourth sensitive IMF to the RMS of the third IMF. The scores for trendability and monotonicity are increased drastically. The trendability and monotonicity are increase to around 0.9 from around 0.2 and 0.5, respectively. The degradation paths for these six data sets from the normal state to the failure state seem practical and similar.

5.3 Further work

Some of the recommendations for further work are listed as follows.

1. The data set is not enough for the analysis and to make a decision. So, more experiments are necessary to run to get more data sets.
2. Some improvements in the data collection system will improve the quality of the collected data sets. Improvement can be done by collecting data samples automatically in the defined time interval. So, the sample interval will be the same all the time. In my view, the most important amendment needed to carry out is the way of pouring the contaminated lubricant into the testing bearing. The way of pouring should be automatic action which can pour a nearly equal amount of lubricant all the time without dropping and spilling.
3. A degradation model shall be developed by using the selected health indicator and predict the remaining useful life of the bearing.
4. In this study, the threshold is only indicated according to the amplitude of the vibration signal. It would be better if the failure threshold as per the value of optimal features can be calculated. It will be a more realistic model.
5. Some machine learning techniques can be trained with the optimal features extracted from the signal processing as an input for better diagnosis and prognosis of the bearings.

Appendix

Appendix A

Acronyms

CBM Condition-Based Maintenance

EMD Empirical Mode Decomposition

EEMD Ensemble Empirical Mode Decomposition

FFT Fast Fourier Transform

HT Hilbert Transform

HHT Hilbert-Huang transform

IMF intrinsic mode functions

NTNU Norwegian University of Science and Technology

RAMS Reliability, Availability, Maintainability, and Safety

RMS Root Means Square

RUL Remaining Useful Life

STFT Short-Time Fourier Transform

WT Wavelet Transform

Appendix B

Experiment record form.

Experiment form

Bearing No.		7		Date	30.12.2020	
Activity	Start time	End time	Reason			
1	10:00	16:00	leaving			
2	11:15	12:51	End of experiment			
3						
Time interval			5 min			
Number of samples			84			
Stress level (Target stress shall be marked)						
Speed		Size of silicon			Density of silicon	
2975 rpm		S M L			Written on the next page	
Stress change log						
	Time		Time		Time	
1						
2						
3						
4						
5						
6						
Summary						
Highest acceleration amplitude					Lowest acceleration amplitude	
Note		Acceleration signals over time (vertical direction)			Vibration signals over frequency (vertical direction)	
		Threshold was 10g for both directions				
Number of data file		84		Prepared by		Kishan prajapati

Experiment form

Bearing failure photo

Notes:

The first 20 samples are taken without applying silicium carbide to get the signature of the signals.

Small = VS 44. D50 – 52 Coultex particles

Medium =

Large =

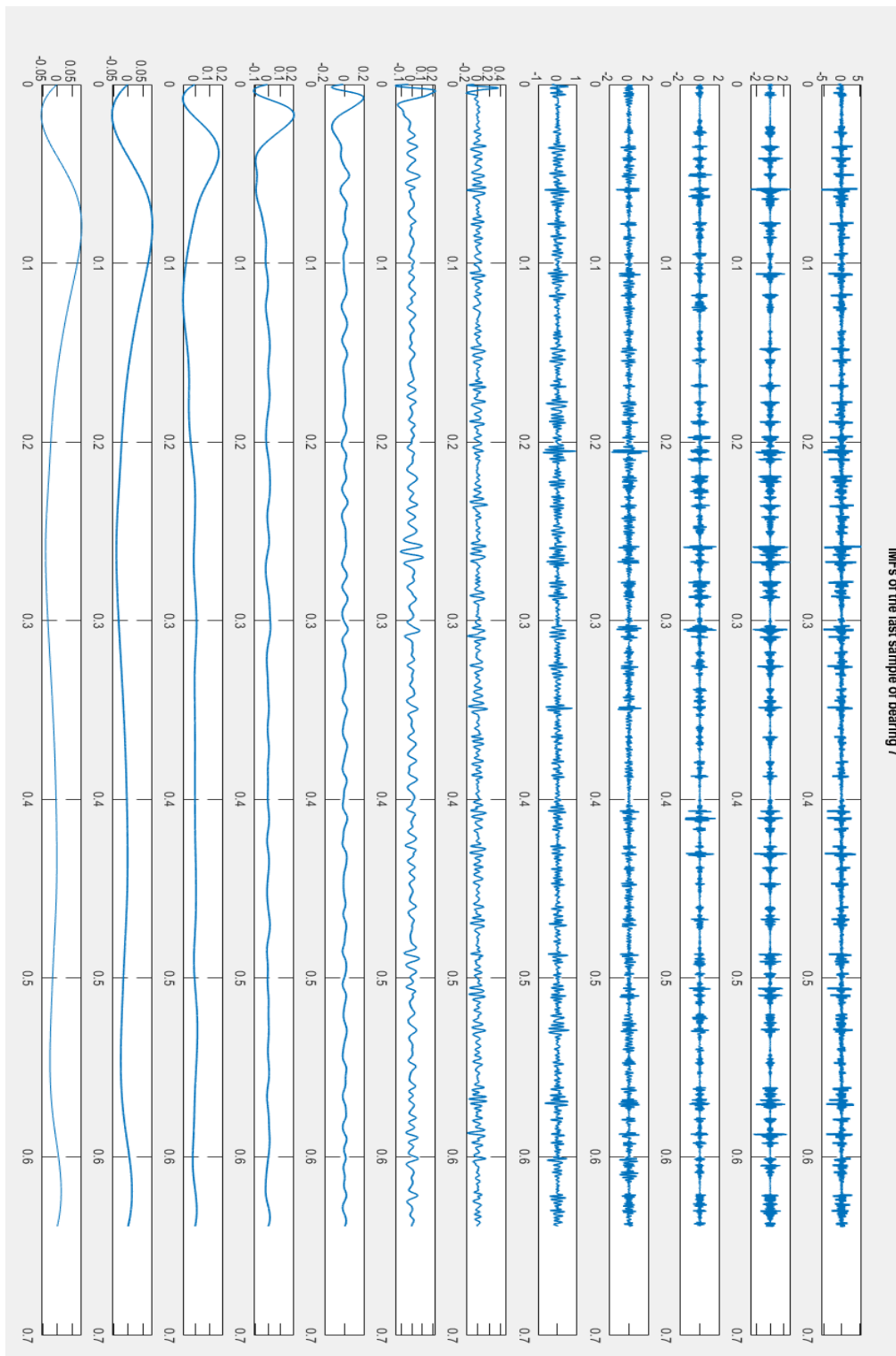
Explantations :

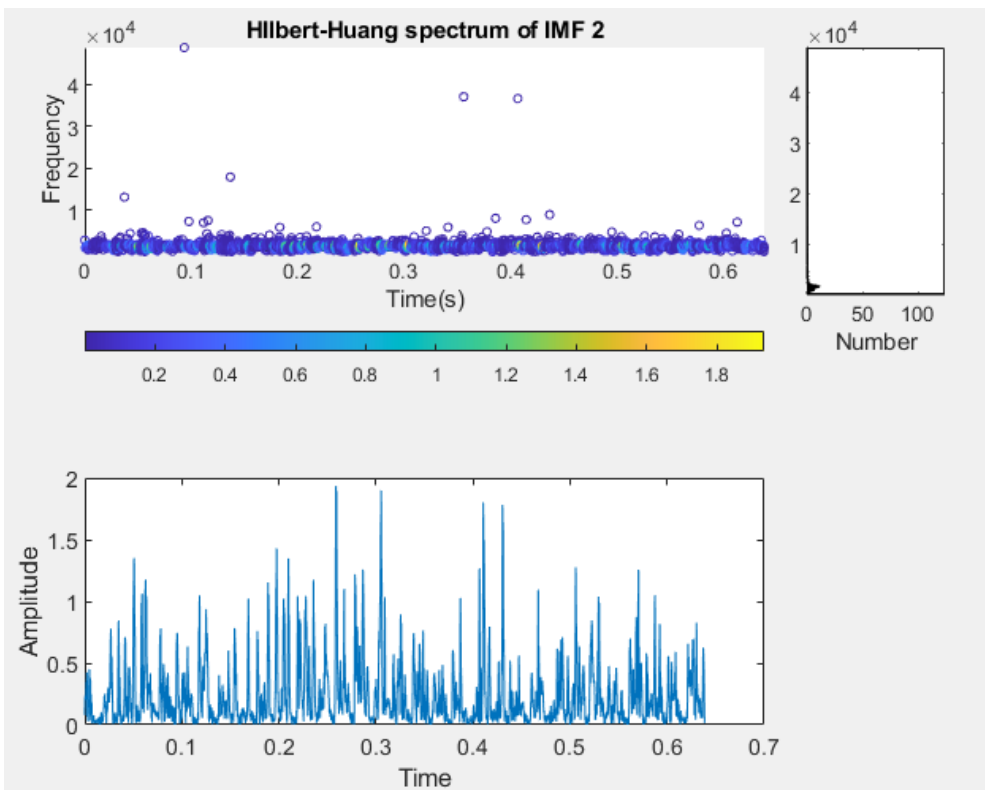
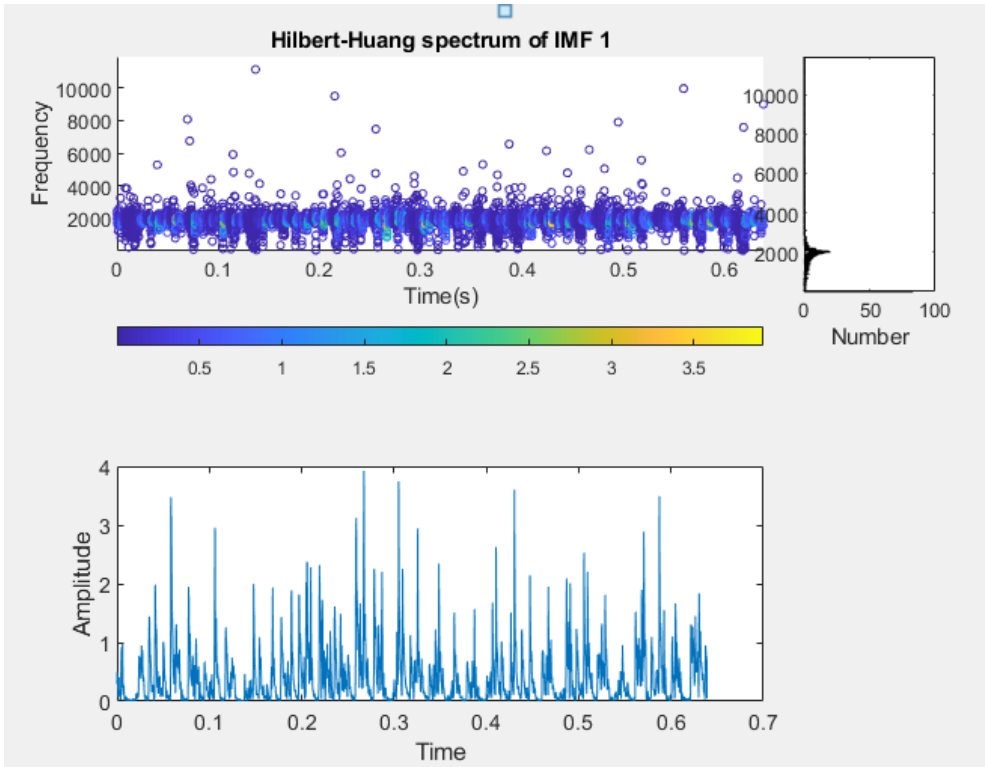
- Weight of the plastic lid that contains the new bearings: 22.7 grains
- Small particles with the lid: 61.7 grains
- Particle weight: 61.7 – 22.7 grains
- Oil weight is the summation of the values written below:
- $275.2 - 22.7 = 252.5$
- $323.2 - 22.7 = 209.5$
- $317.2 - 22.7 = 295.5$
- $279.1 - 22.7 = 256.4$
- $246.2 - 22.7 = 223.5$
- $274.8 - 22.7 = 252.1$

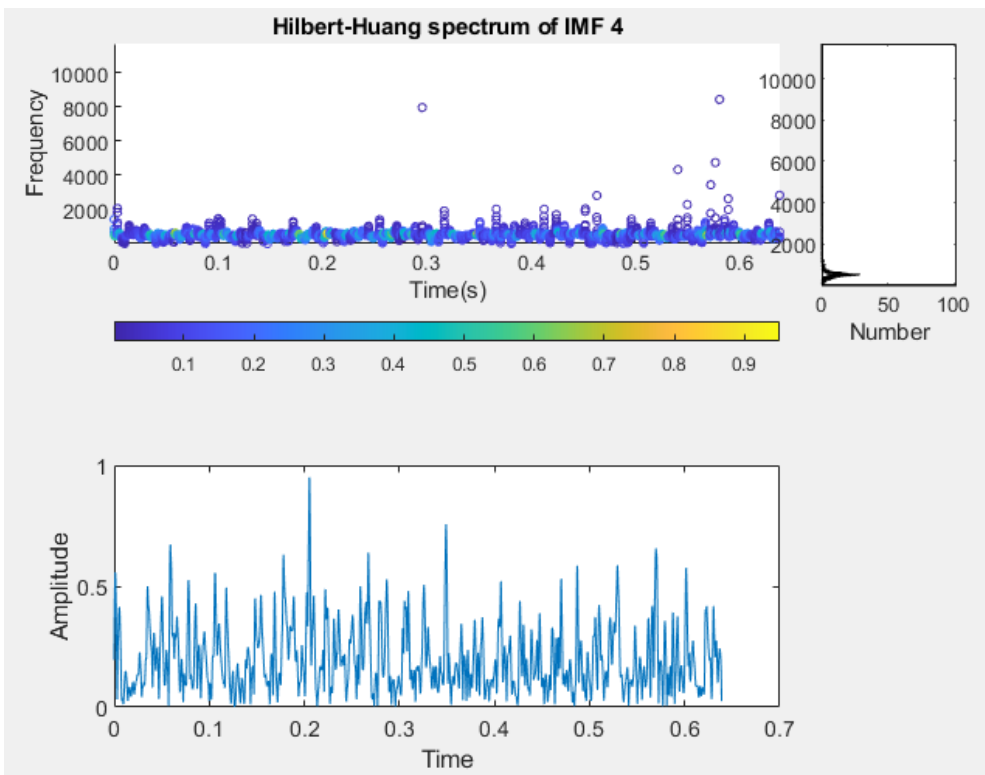
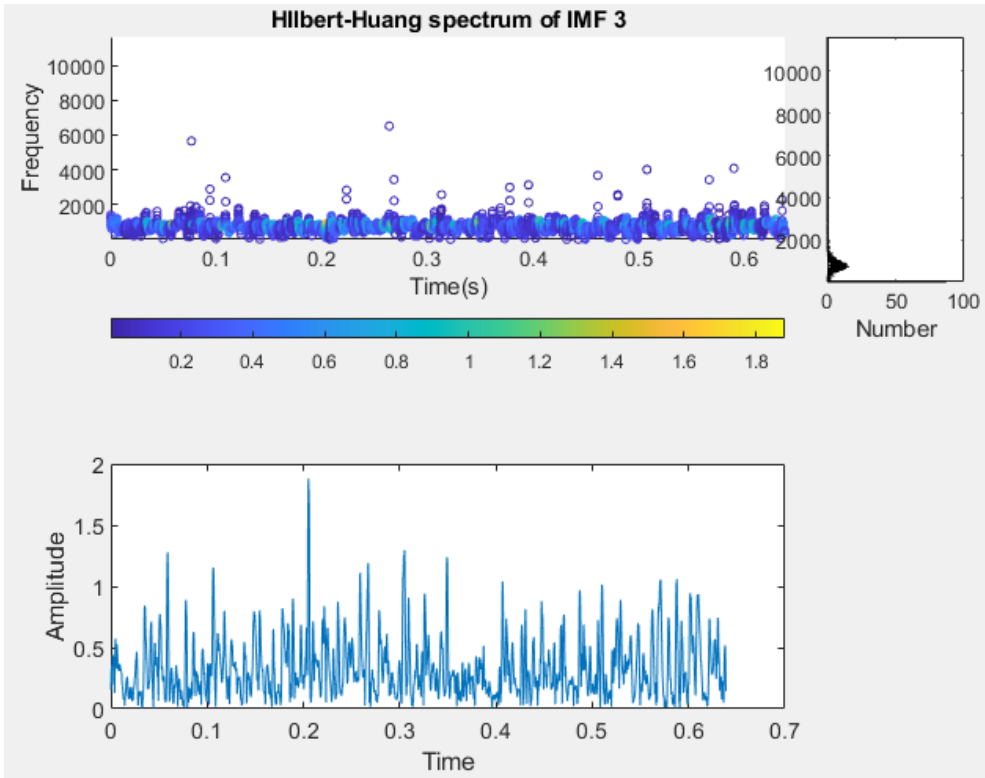
Appendix B

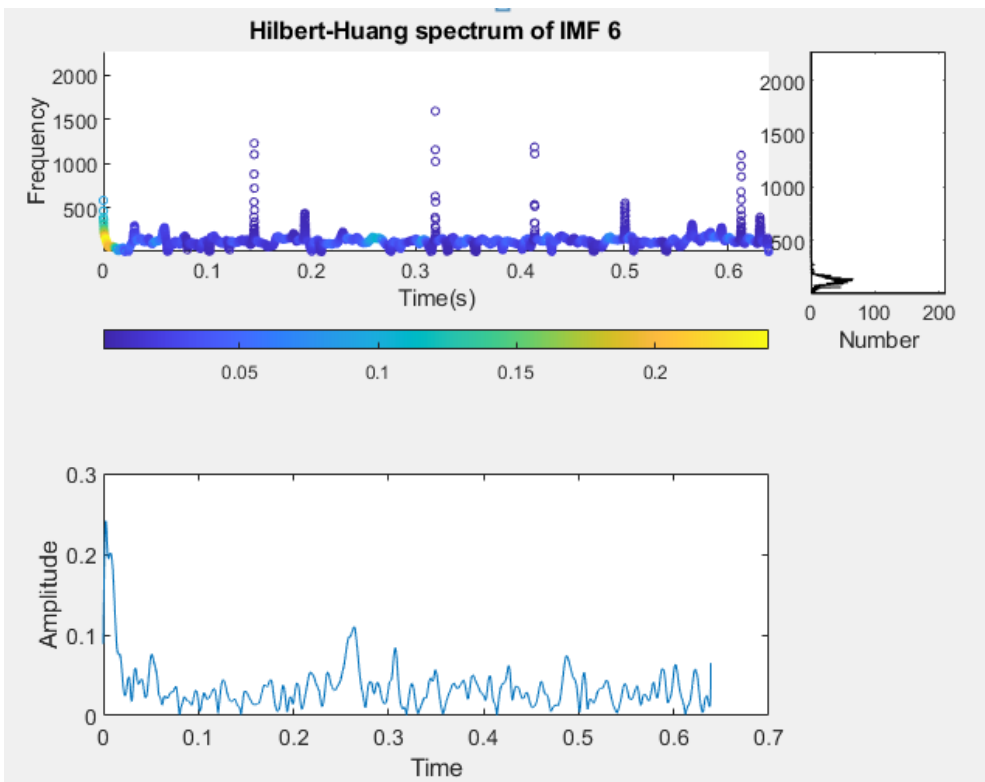
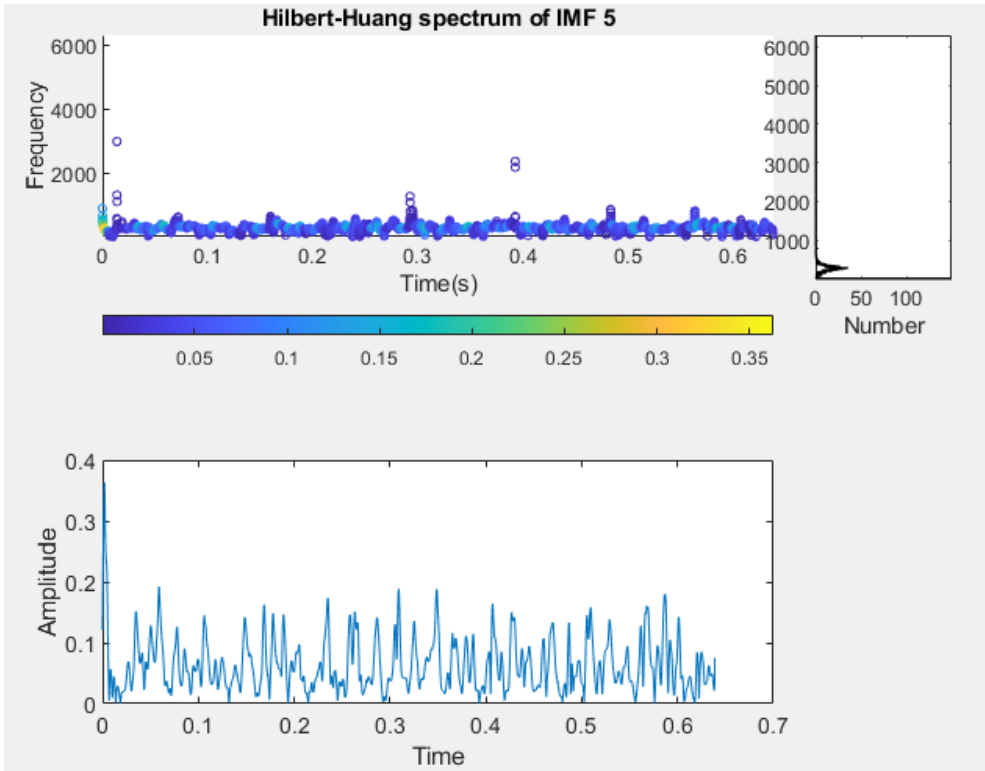
Intrinsic mode decomposition (IMF) and Hilbert-Huang spectrum

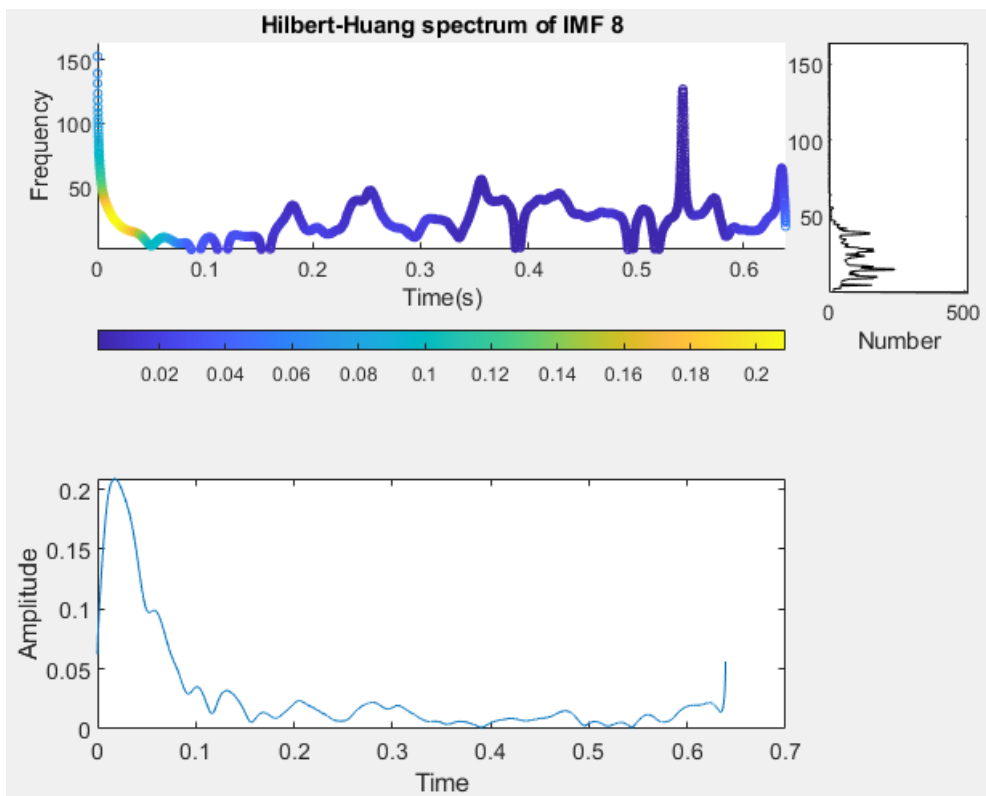
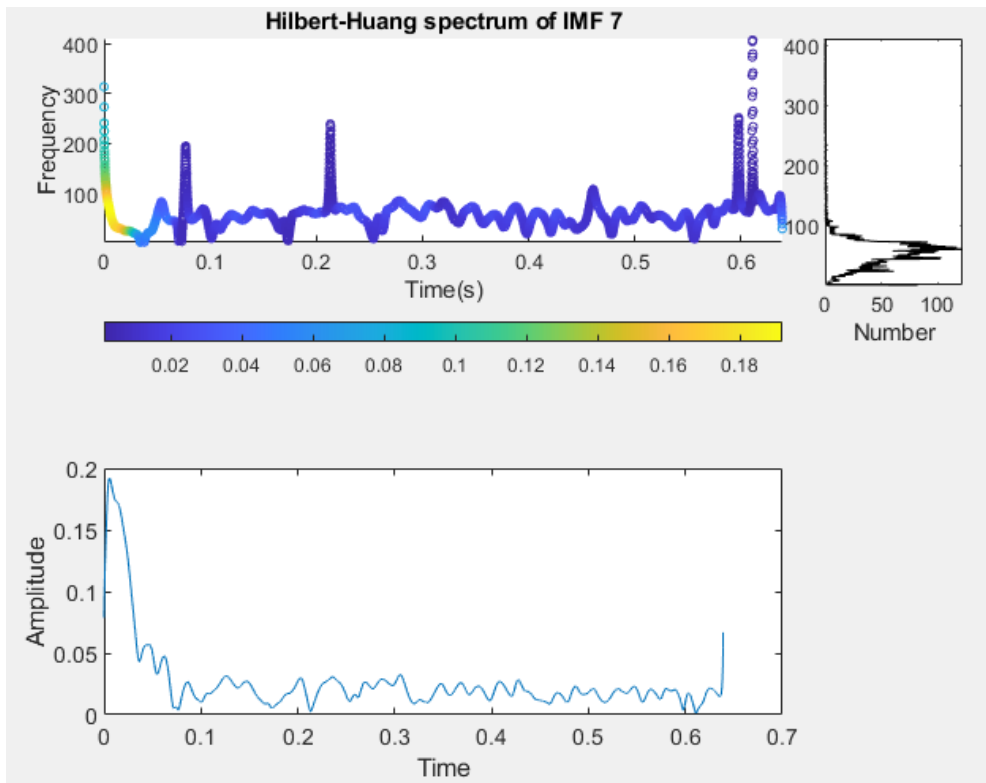
The decomposition of last sample of bearing 7 using EEMD. The results are IMFs and the Hilbert-Huang spectrum of the first eight IMFs as displayed as follows.





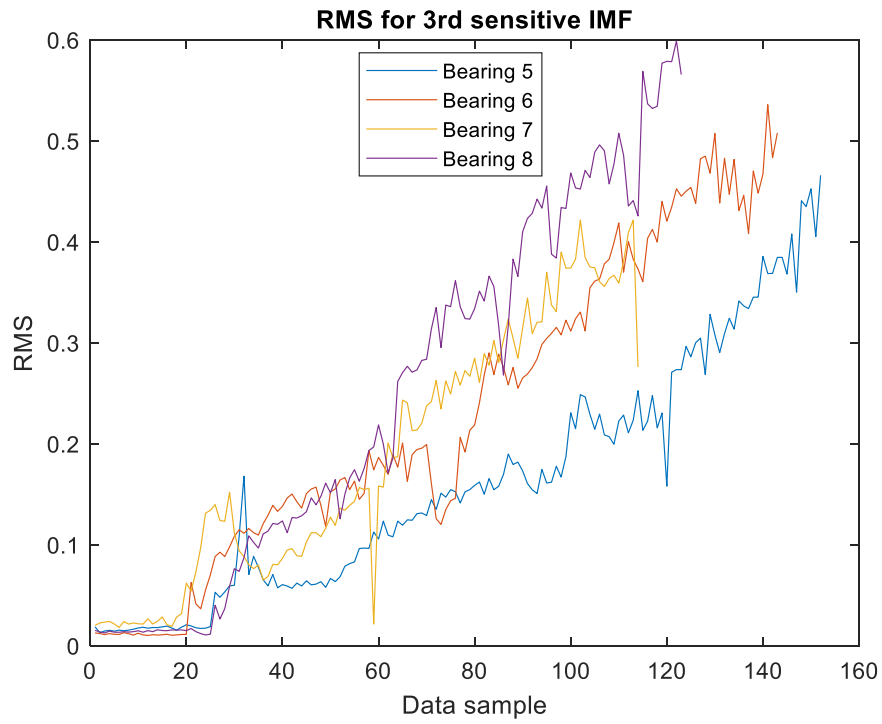






Appendix C

Degradation path for the bearing 5, bearing 6, bearing 7, and bearing 8 represented by RMS for the third sensitive IMF



Reference

- Ayo-Imoru, R. M., & Cilliers, A. C. (2018). A survey of the state of condition-based maintenance (CBM) in the nuclear power industry. *Annals of Nuclear Energy*, *112*, 177-188. <https://doi.org/https://doi.org/10.1016/j.anucene.2017.10.010>
- Bartelmus, W., & Zimroz, R. (2009). A new feature for monitoring the condition of gearboxes in non-stationary operating conditions. *Mechanical Systems and Signal Processing*, *23*(5), 1528-1534.
- Bastami, A. R., & Bashari, A. (2020). Rolling element bearing diagnosis using spectral kurtosis based on optimized impulse response wavelet. *Journal of Vibration and Control*, *26*(3-4), 175-185.
- Batista, L., Badri, B., Sabourin, R., & Thomas, M. (2013). A classifier fusion system for bearing fault diagnosis. *Expert Systems with Applications*, *40*(17), 6788-6797.
- Carden, E. P., & Fanning, P. (2004). Vibration Based Condition Monitoring: A Review. *Structural health monitoring*, *3*(4), 355-377. <https://doi.org/10.1177/1475921704047500>
- Cempel, C., & Tabaszewski, M. (2007). Multidimensional condition monitoring of machines in non-stationary operation. *Mechanical Systems and Signal Processing*, *21*(3), 1233-1241.
- Chen, B., Zhao, S.-l., & Li, P.-y. (2014). Application of Hilbert-Huang transform in structural health monitoring: a state-of-the-art review. *Mathematical Problems in Engineering*, *2014*.
- Chin, H. H., Varbanov, P. S., Klemeš, J. J., Benjamin, M. F. D., & Tan, R. R. (2020). Asset maintenance optimisation approaches in the chemical and process industries – A review. *Chemical Engineering Research and Design*, *164*, 162-194. <https://doi.org/https://doi.org/10.1016/j.cherd.2020.09.034>
- Cohen, L. (1995). *Time-frequency analysis* (Vol. 778). Prentice Hall PTR Englewood Cliffs, NJ.
- Colominas, M. A., Schlotthauer, G., Torres, M. E., & Flandrin, P. (2012). Noise-assisted EMD methods in action. *Advances in adaptive data analysis*, *4*(04), 1250025.
- Cui, L., Huang, J., & Zhang, F. (2017). Quantitative and Localization Diagnosis of a Defective Ball Bearing Based on Vertical-Horizontal Synchronization Signal Analysis [Article]. *IEEE Transactions on Industrial Electronics*, *64*(11), 8695-8706, Article 7913626. <https://doi.org/10.1109/TIE.2017.2698359>
- Feldman, M. (2011). *Hilbert transform applications in mechanical vibration*. John Wiley & Sons.
- Flandrin, P., Rilling, G., & Goncalves, P. (2004). Empirical mode decomposition as a filter bank. *IEEE signal processing letters*, *11*(2), 112-114.
- Houcque, D. (2005). *INTRODUCTION TO MATLAB FOR ENGINEERING STUDENTS*. <https://www.mccormick.northwestern.edu/documents/students/undergraduate/introduction-to-matlab.pdf>
- Huang, N., & Busalacchi, A. J. (2000). A new view of earthquake ground motion data: the Hilbert spectral analysis.
- Huang, N. E., Shen, Z., & Long, S. R. (1998). The empirical mode decomposition and the Hilbert spectrum for nonlinear and non-stationary time series analysis. *The Empirical Mode*

Decomposition and the Hilbert Spectrum for Nonlinear and Non-Stationary Time Series Analysis, 903-995.

- Huang, N. E., Shen, Z., & Long, S. R. (1999). A new view of nonlinear water waves: the Hilbert spectrum. *Annual review of fluid mechanics*, 31(1), 417-457.
- IEEE Motor Reliability Working Group. (1985). Report of Large Motor Reliability Survey of Industrial and Commercial Installations, Part I. *IEEE Transactions on Industry Applications*, IA-21(4), 853-864. <https://doi.org/10.1109/TIA.1985.349532>
- Jardine, A. K. S., Lin, D., & Banjevic, D. (2006). A review on machinery diagnostics and prognostics implementing condition-based maintenance. *Mechanical Systems and Signal Processing*, 20(7), 1483-1510. <https://doi.org/https://doi.org/10.1016/j.ymsp.2005.09.012>
- Junsheng, C., Dejie, Y., & Yu, Y. (2005). Time–energy density analysis based on wavelet transform. *Ndt & E International*, 38(7), 569-572.
- KiranKumar, M., Loksha, M., Kumar, S., & Kumar, A. (2018). Review on Condition Monitoring of Bearings using vibration analysis techniques. IOP Conference Series: Materials Science and Engineering,
- Lei, Y. (2016). *Intelligent Fault Diagnosis and Remaining Useful Life Prediction of Rotating Machinery* (1 ed.). Oxford: Elsevier Science & Technology.
- Lei, Y., He, Z., & Zi, Y. (2011). EEMD method and WNN for fault diagnosis of locomotive roller bearings. *Expert Systems with Applications*, 38(6), 7334-7341. <https://doi.org/https://doi.org/10.1016/j.eswa.2010.12.095>
- Lei, Y., Lin, J., Han, D., & He, Z. (2014). An enhanced stochastic resonance method for weak feature extraction from vibration signals in bearing fault detection. *Proceedings of the Institution of Mechanical Engineers, Part C: Journal of Mechanical Engineering Science*, 228(5), 815-827. <https://doi.org/10.1177/0954406213492067>
- Lei, Y., Lin, J., He, Z., & Zuo, M. J. (2013). A review on empirical mode decomposition in fault diagnosis of rotating machinery. *Mechanical Systems and Signal Processing*, 35(1), 108-126. <https://doi.org/https://doi.org/10.1016/j.ymsp.2012.09.015>
- Lei, Y., Liu, Z., Ouazri, J., & Lin, J. (2015). A fault diagnosis method of rolling element bearings based on CEEMDAN.
- Lei, Y., & Zuo, M. J. (2009). Fault diagnosis of rotating machinery using an improved HHT based on EEMD and sensitive IMFs. *Measurement Science and Technology*, 20(12), 125701.
- Li, B., Xie, W.-C., & Pandey, M. D. (2016). Generate tri-directional spectra-compatible time histories using HHT method. *Nuclear Engineering and Design*, 308, 73-85.
- Liu, H., & Han, M. (2014). A fault diagnosis method based on local mean decomposition and multi-scale entropy for roller bearings. *Mechanism and Machine Theory*, 75, 67-78. <https://doi.org/https://doi.org/10.1016/j.mechmachtheory.2014.01.011>
- Liu, J. (2020). *Maintenance models for real time optimization of wind farm maintenance* [Academic, Norwegian University of Science and Technology]. Trondheim, Norway.
- Liu, Z., Cao, H., Chen, X., He, Z., & Shen, Z. (2013). Multi-fault classification based on wavelet SVM with PSO algorithm to analyze vibration signals from rolling element bearings. *Neurocomputing*, 99, 399-410. <https://doi.org/https://doi.org/10.1016/j.neucom.2012.07.019>
- Lou, M., & Huang, T. (2007). Orthogonal empirical mode decomposition [J]. *Journal of Tongji University (Natural Science)*, 3(35), 3.
- Lou, X., & Loparo, K. A. (2004). Bearing fault diagnosis based on wavelet transform and fuzzy inference. *Mechanical Systems and Signal Processing*, 18(5), 1077-1095.

- Loughlin, P. J., Pitton, J. W., & Atlas, L. E. (1992). Proper time-frequency energy distributions and the Heisenberg uncertainty principle. [1992] Proceedings of the IEEE-SP International Symposium on Time-Frequency and Time-Scale Analysis,
- Loutridis, S. J. (2006). Instantaneous energy density as a feature for gear fault detection. *Mechanical Systems and Signal Processing*, 20(5), 1239-1253. <https://doi.org/https://doi.org/10.1016/j.ymssp.2004.12.001>
- Mathew, J., & Alfredson, R. (1984). The condition monitoring of rolling element bearings using vibration analysis.
- MathWorks. (2021). *MathWorks*. <https://se.mathworks.com/>
- Mechefske, C. K. (2005). Machine condition monitoring and fault diagnostics. In *Vibration and Shock Handbook* (Vol. 25, pp. 1-35). CRC Press, Taylor and Francis Group Boca Raton, FL.
- Meltzer, G., & Dien, N. P. (2004). Fault diagnosis in gears operating under non-stationary rotational speed using polar wavelet amplitude maps. *Mechanical Systems and Signal Processing*, 18(5), 985-992.
- Montesinos, M., Munoz-Cobo, J., & Perez, C. (2003). Hilbert–Huang analysis of BWR neutron detector signals: application to DR calculation and to corrupted signal analysis. *Annals of Nuclear Energy*, 30(6), 715-727.
- Motahari-Nezhad, M., & Jafari, S. M. (2021). Bearing remaining useful life prediction under starved lubricating condition using time domain acoustic emission signal processing. *Expert Systems with Applications*, 168, 114391. <https://doi.org/https://doi.org/10.1016/j.eswa.2020.114391>
- Nayana, B., & Geethanjali, P. (2017). Analysis of statistical time-domain features effectiveness in identification of bearing faults from vibration signal. *IEEE Sensors Journal*, 17(17), 5618-5625.
- Nithyavathy, N., Kumar, S. A., Sheriff, K. A. I., Hariram, A., & Prasaad, P. H. (2021). Vibration monitoring and analysis of ball bearing using GSD platform. *Materials Today: Proceedings*. <https://doi.org/https://doi.org/10.1016/j.matpr.2020.12.1088>
- Ondra, V., Sever, I. A., & Schwingshackl, C. W. (2021). Identification of complex non-linear modes of mechanical systems using the Hilbert-Huang transform from free decay responses. *Journal of Sound and Vibration*, 495, 115912. <https://doi.org/https://doi.org/10.1016/j.jsv.2020.115912>
- Patel, A., & Shakya, P. (2020). Early fault detection based on empirical mode decomposition method. *Procedia CIRP*, 88, 31-35. <https://doi.org/https://doi.org/10.1016/j.procir.2020.05.006>
- Patil, M., Mathew, J., & RajendraKumar, P. (2008). Bearing signature analysis as a medium for fault detection: a review. *Journal of Tribology*, 130(1).
- Peng, Z., Chu, F., & He, Y. (2002). VIBRATION SIGNAL ANALYSIS AND FEATURE EXTRACTION BASED ON REASSIGNED WAVELET SCALOGRAM. *Journal of Sound and Vibration*, 253(5), 1087-1100. <https://doi.org/https://doi.org/10.1006/jsvi.2001.4085>
- Peng, Z., Peter, W. T., & Chu, F. (2005a). A comparison study of improved Hilbert–Huang transform and wavelet transform: application to fault diagnosis for rolling bearing. *Mechanical Systems and Signal Processing*, 19(5), 974-988.
- Peng, Z., Peter, W. T., & Chu, F. (2005b). An improved Hilbert–Huang transform and its application in vibration signal analysis. *Journal of Sound and Vibration*, 286(1-2), 187-205.

- Peng, Z. K., Tse, P. W., & Chu, F. L. (2005). A comparison study of improved Hilbert–Huang transform and wavelet transform: Application to fault diagnosis for rolling bearing. *Mechanical Systems and Signal Processing*, 19(5), 974-988. <https://doi.org/https://doi.org/10.1016/j.ymssp.2004.01.006>
- Phan, S. K., & Chen, C. (2017). Big data and monitoring the grid. In B. W. D’Andrade (Ed.), *The Power Grid Smart, Secure, Green and Reliable* (pp. 253-285). Academic Press.
- Qin, X., Li, Q., Dong, X., & Lv, S. (2017). The fault diagnosis of rolling bearing based on ensemble empirical mode decomposition and random forest. *Shock and Vibration*, 2017.
- Qiu, G., Gu, Y., & Chen, J. (2020). Selective health indicator for bearings ensemble remaining useful life prediction with genetic algorithm and Weibull proportional hazards model. *Measurement*, 150, 107097. <https://doi.org/https://doi.org/10.1016/j.measurement.2019.107097>
- Rai, A., & Upadhyay, S. H. (2016). A review on signal processing techniques utilized in the fault diagnosis of rolling element bearings. *Tribology international*, 96, 289-306. <https://doi.org/https://doi.org/10.1016/j.triboint.2015.12.037>
- Rato, R., Ortigueira, M. D., & Batista, A. (2008). On the HHT, its problems, and some solutions. *Mechanical Systems and Signal Processing*, 22(6), 1374-1394.
- Song, L., Liang, H., Teng, W., & Guo, L. (2019). Health indicator construction and remaining useful life prediction for space Stirling cryocooler. *Advances in Mechanical Engineering*, 11(12), 1687814019896734.
- Sun, Y., Li, S., & Wang, X. (2021). Bearing fault diagnosis based on EMD and improved Chebyshev distance in SDP image. *Measurement*, 176, 109100. <https://doi.org/https://doi.org/10.1016/j.measurement.2021.109100>
- Tahir, M. M., Badshah, S., Hussain, A., & Khattak, M. A. (2017). Extracting accurate time domain features from vibration signals for reliable classification of bearing faults. *Int. J. Adv. Appl. Sci*, 5(1), 156-163.
- Tajiani, B., & Vatn, J. (2021). RUL Prediction of Bearings using Empirical Wavelet Transform and Bayesian Approach.
- Tajiani, B., Vatn, J., & Pedersen, V. G. B. (2020). Remaining Useful Life Estimation Using Vibration-based Degradation Signals. 8.
- Tandon, N., & Choudhury, A. (1999). A review of vibration and acoustic measurement methods for the detection of defects in rolling element bearings. *Tribology international*, 32(8), 469-480. [https://doi.org/10.1016/S0301-679X\(99\)00077-8](https://doi.org/10.1016/S0301-679X(99)00077-8)
- Urbanek, J., Barszcz, T., Zimroz, R., & Antoni, J. (2012). Application of averaged instantaneous power spectrum for diagnostics of machinery operating under non-stationary operational conditions. *Measurement*, 45(7), 1782-1791.
- Verma, A., Zhang, Z., & Kusiak, A. (2013). Modeling and prediction of gearbox faults with data-mining algorithms. *Journal of solar energy engineering*, 135(3).
- Vishwakarma, M., Purohit, R., Harshlata, V., & Rajput, P. (2017). Vibration Analysis & Condition Monitoring for Rotating Machines: A Review. *Materials Today: Proceedings*, 4(2, Part A), 2659-2664. <https://doi.org/https://doi.org/10.1016/j.matpr.2017.02.140>
- Wang, D., Guo, W., & Tse, P. W. (2016). An enhanced empirical mode decomposition method for blind component separation of a single-channel vibration signal mixture. *Journal of Vibration and Control*, 22(11), 2603-2618.
- Wang, H.-d., Deng, S.-e., Yang, J.-x., & Liao, H. (2019). A fault diagnosis method for rolling element bearing (REB) based on reducing REB foundation vibration and noise-assisted

- vibration signal analysis. *Proceedings of the Institution of Mechanical Engineers, Part C: Journal of Mechanical Engineering Science*, 233(7), 2574-2587.
- Wu, M.-C., & Huang, N. E. (2009). Biomedical Data Processing Using HHT: A Review. In A. Naït-Ali (Ed.), *Advanced Biosignal Processing* (pp. 335-352). Springer Berlin Heidelberg. https://doi.org/10.1007/978-3-540-89506-0_16
- Wu, Z., & Huang, N. E. (2004). A study of the characteristics of white noise using the empirical mode decomposition method. *Proceedings of the Royal Society of London. Series A: mathematical, physical and engineering sciences*, 460(2046), 1597-1611.
- Wu, Z., & Huang, N. E. (2009). Ensemble empirical mode decomposition: a noise-assisted data analysis method. *Advances in adaptive data analysis*, 1(01), 1-41.
- Xiao, W., Chen, J., Dong, G., Zhou, Y., & Wang, Z. (2012). A multichannel fusion approach based on coupled hidden Markov models for rolling element bearing fault diagnosis. *Proceedings of the Institution of Mechanical Engineers, Part C: Journal of Mechanical Engineering Science*, 226(1), 202-216.
- Xu, Y., Zhang, K., Ma, C., Cui, L., & Tian, W. (2019). Adaptive Kurtogram and its applications in rolling bearing fault diagnosis. *Mechanical Systems and Signal Processing*, 130, 87-107. <https://doi.org/https://doi.org/10.1016/j.ymssp.2019.05.003>
- Yang, H., Ning, T., Zhang, B., Yin, X., & Gao, Z. (2017). An adaptive denoising fault feature extraction method based on ensemble empirical mode decomposition and the correlation coefficient. *Advances in Mechanical Engineering*, 9(4), 1687814017696448.
- Yinfeng, D., Yingmin, L., Mingkui, X., & Ming, L. (2008). Analysis of earthquake ground motions using an improved Hilbert–Huang transform. *Soil Dynamics and Earthquake Engineering*, 28(1), 7-19.
- Yong, Y., Shuai, Z., & Yanhuai, Q. (2011, 15-17 July 2011). The method of vibration Fault Detection and diagnosis in rotor systems based on Hilbert-Huang Transform. 2011 Second International Conference on Mechanic Automation and Control Engineering,
- Yu, Y., & Junsheng, C. (2006). A roller bearing fault diagnosis method based on EMD energy entropy and ANN. *Journal of Sound and Vibration*, 294(1-2), 269-277.
- Zhang, K., Ma, C., Xu, Y., Chen, P., & Du, J. (2021). Feature extraction method based on adaptive and concise empirical wavelet transform and its applications in bearing fault diagnosis. *Measurement*, 172, 108976. <https://doi.org/https://doi.org/10.1016/j.measurement.2021.108976>

